THE PRESENCE OF NAKED PURKINJE CELL DENDRITIC SPINE SPECIALIZATIONS AND OTHER PATHOLOGICAL CHANGES IN TEN DAY SALINE AND METHYLAZOXYMETHANOL - INJECTED SWISS ALBINO MICE

Thesis for the Degree of M. S.

MICHIGAN STATE UNIVERSITY

THOMAS H. HARTKOP

1976

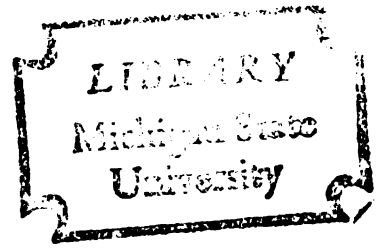

ABSTRACT

THE PRESENCE OF NAKED PURKINJE CELL DENDRITIC SPINE SPECIALIZATIONS AND OTHER PATHOLOGICAL CHANGES IN TEN DAY SALINE AND METHYLAZOXYMETHANOL-INJECTED SWISS ALBINO MICE

By

Thomas Henry Hartkop

Postnatal Swiss albino mice, Webster strain, treated at day zero with methylazoxymethanol acetate (MAM) or saline 0.05 ul/gm body weight, were sacrificed at 10 days of age. Attention was directed towards the differentiation of synaptic structures as well as to physical, histological and ultrastructural alterations. Naked Purkinje cell dendritic spines with postsynaptic spine specializations were observed in both control and treated ten postnatal day mice. Many granule cells in their definitive locations exhibited parallel fiber-Purkinje cell contacts. A planimetric evaluation of the midsagittal surface area of the vermis revealed an average reduction of 60% in the MAM-treated mice. Dislocation of Purkinje cell somata, random orientation of their apical poles and alterations within the Purkinje cell dendrites in 10 day MAM-treated mice were observed. The vertical processes of the Golgi epithelial

(Bergmann) cells were reduced in length passed in an oblique direction towards the meninges, and contained fewer than normal warty excrescences. Necrotic debris was observed within the external differentiating cell layer in 10 day MAM-injected mice. No evidence of degeneration of pre-synaptic terminals was observed in either group.

This study would appear to strengthen the hypothesis that Purkinje cell dendritic spine specializations do not require permanent presynaptic contact by parallel fibers for development.

THE PRESENCE OF NAKED PURKINJE CELL DENDRITIC SPINE SPECIALIZATIONS AND OTHER PATHOLOGICAL CHANGES IN TEN DAY SALINE AND METHYLAZOXYMETHANOL-INJECTED SWISS ALBINO MICE

by

Thomas H. Hartkop

A THESIS

Submitted to
Michigan State University
in partial fulfillment of the requirements
for the degree of

MASTER OF SCIENCE

Department of Anatomy

1976

DEDICATION

I dedicate this manuscript to my wife, Michele, my mother, Georgina R. Hartkop, and to the memory of my father, Dr. Henry H. Hartkop.

ACKNOWLEDGMENTS

I wish to express my sincere thanks to my major Professors, Dr. Thomas W. Jenkins and Dr. Margaret Z. Jones for their guidance and friendship during the past years. Appreciation is also due to Dr. Lawrence M. Ross and Dr. John E. Wilson for serving on my committee.

I would like to also thank Donna Craft, Mary E. Gardner, Mrs. Nina Miller, Denise I. Stanke and Warren Taylor for their technical advice and assistance and my wife Michele A. Hartkop and Rebecca McMahon for typing and proofreading preliminary drafts of this manuscript.

TABLE OF CONTENTS

LIST OF FIGURES

List of figures continued

LIST OF CHARTS

INTRODUCTION

The cerebellar cortex is an excellent subject for experimentation because of its histological homogeneity, and the recent advances in knowledge regarding its normal development. Moreover, the synaptic architecture of the cerebellum has been delineated from both morphological and functional standpoints. Thus, cerebellar elements and their synaptic contacts can be studied with some measure of confidence (Hirano and Zimmerman, 1973).

During the development of the cerebellar cortex, differentiated cells migrate from the external differentiating cell layer and assume their definitive locations as internal granule, stellate or basket cells. Ultrastructurally, granule cells that have completed their migration into the internal granule cell layer have left behind, during their excursion, an unmyelinated ascending axon that passes into the molecular layer to its point of bifurcation. From the point of bifurcation, parallel fibers are thereby developed in a plane parallel to the folial surface with numerous varicosities, containing synaptic vesicles, that make synaptic contact with the Purkinje cell dendritic spine specializations, basket, stellate, or Golgi II dendrites (Palay and Chan-Palay, 1974; Herndon, 1964; del Cerro and Snider, 1972; Larramendi, 1969). Larramendi (1969) described the development of parallel fiber-Purkinje cell dendritic spine synapses within the upper molecular layer of 14 day old mice. He

stated that pre- and postsynaptic specializations form after the pre- and postsynaptic elements have fused. Subsequent to Larramendi's (1969) report, the deletion of presynaptic elements by a variety of pathological processes has been shown to lead to the differentiation of naked Purkinje cell dendritic spine specializations (Altman and Anderson, 1972, 1973; Herndon, Margolis, and Kilham, 1971; Herndon, 1968; Llinas, Hillman and Precht, 1972; Hirano and Dembitzer, 1973, 1975; Hirano and Jones, 1972; Hirano, Dembitzer and Jones, 1972; Mouren-Mathieu and Colonnier, 1969, Sotelo, 1973, 1975). Cycasin (methylazoxymethanol glucoside) and MAM (methylazoxymethanol acetate), the agent used in this study, have been shown to destroy actively dividing cells within the external differentiating cell layer when injected into mice, rats, or hamsters, resulting in a decrease in parallel fibers and their synaptic contacts (Hirano, et al., 1972; Hirano and Jones, 1972; Jones, Yang and Michelsen, 1972a; Jones, Michelsen and Yang, 1973). Concomitantly with aberrant synaptogenesis, the administration of MAM results in physical, histological and ultrastructural alterations by the tenth postnatal day. Such changes can be monitored by assessing the physical maturity, macroscopic changes within the cerebellar vermis, and histological alterations in the cerebellar cortex of 10 day treated and control mice. Questions concerning synaptogenesis such as the development and durability of the naked

Purkinje cell dendritic spine specializations which result from MAM treatment, can be addressed by comparison of similarities and differences of ultrastructural characteristics of MAM and saline groups.

The physical and behavioral maturity of zero day cycasin-treated mice has been previously reported at different postnatal ages (Jones, et al., 1973). In this experiment, sixty percent of 70 treated mice exhibited some aberrant physical, motor or postural changes, sometime during their initial 25 postnatal days. Recovery of function occurred in less severely affected animals even though the cerebellum was severely damaged (Jones, et al., 1973). Studies in genetic mutants have shown an appearance of cerebellar dysfunction before synaptogenesis is completed in the Weaver mouse (Rakic and Sidman, 1973c). These studies have supported the need for assessments of physical and behavioral characteristics like those carried out in this investigation.

The definitive histologic changes seen in MAM-injected mice consist of destruction within the external differentiating cell layer, which causes a concomitant decrease in the foliation in midsagittal sections of the cerebellum (Chanda, et al., 1973; Jones, et al., 1972a, 1973; Woodward, et al., 1975). A reduction in the size of the vermis has also been observed in animals subjected to a virus infection of feline panleukopenia (Herndon, et al.,

1971, Llinas, et al., 1972), genetic defects (Caddy and Biscoe, 1975; Hirano and Dembitzer, 1975; Rakic and Sidman, 1973b, 1973c), and x-irradiation in rats (Altman and Anderson, 1971, 1972; Altman, et al., 1971; Anderson and Altman, 1971). A planimetric evaluation of the midsagittal sections of the vermis in rats was made by Woodward, et al. (1975). This method was used to compare the size reductions observed in midsagittal sections of the vermis in 10 day MAM injected mice and the size reductions previously reported in treated rats. Modifications of this method were used in this study to document the extent of external differentiating cell layer destruction after MAM treatment.

Random dislocation of Purkinje cell somata has been shown in animals that have exhibited an external differentiating and internal granule cell loss due to genetic defects (Hirano and Dembitzer, 1975; Rakic and Sidman, 1973b; Sax, Hirano and Shofer, 1968), virus infection with feline panleukopenia (Herndon, et al., 1971; Llinas, et al., 1972), x-ray (Altman and Anderson, 1971, 1972; Altman, Anderson, and Strop, 1971; Anderson and Altman, 1971), and MAM-treatment (Chanda, Woodward and Griffin, 1973; Herndon, et al., 1971; Jones, et al., 1972a, 1973; Shimada and Langman, 1970; Woodward, et al., 1975). Various theories have been proposed to explain the Purkinje cell apical pole orientation observed in 10 day saline and MAM-injected mice.

With respect to number and orientation, changes in Purkinje cell primary dendrites have been described. Woodward, et al. (1975) suggested a plausible hypothesis for the formation of multiple primary dendrites. The presence of many massive Purkinje cell primary dendrites in MAM-injected mice will be discussed in relation to this hypothesis. The altered number and random three dimensional orientation of secondary and tertiary branches and branchlets with spines on Purkinje cell somata have been previously reported in a variety of animals (Altman and Anderson, 1971, 1972b, 1972d; Hamori, 1969; Mouren-Mathieu and Colonnier, 1969; Shofer, Pappas, and Purpura, 1964; Woodward, et al., 1975). The Purkinje cell dendrite and its dendritic processes will be described after MAM treatment.

In a developmental and comparative light microscopic study, Swiss albino mice were injected with cycasin (0.5 mg/gm body weight), MAM (0.05 ul/gm body weight) or physiological saline (0.05 ul/gm body weight) within the first 24 hours after birth. As early as six hours after injection with the MAM, cellular necrosis was evident within the external differentiating cell layer. Cycasin and MAM-injected mice both exhibited extensive necrosis in the external differentiating cell layer by two days post-injection. By the fifth post-injection day, both the external differentiating and internal granule cell layers

were markedly diminished, while the misaligned Purkinje cells were scattered in the molecular layer (Jones, et al., 1972a, 1973). External differentiating cells that escape MAM-destruction may undergo prolific regeneration to replenish the external differentiating cell layer. The cells within this layer will eventually migrate inward to repopulate the internal granular cell layer (Chanda, et al., 1973; Shimada and Langman, 1970; Woodward, et al., 1975). The previously described destruction as well as the presence of persistent necrotic debris, and subsequent regeneration within the cerebellar cortex will be discussed and contrasted to that observed in the 10 day MAM-injected mice.

Bergmann fibers appear to be implicated in the migration of differentiating granule cells by maintaining a side-by-side aposition, thereby directing the granule cells toward their definitive location in the internal cell layer (Rakic, 1971; Sotelo and Chargeux, 1974). Anatomical variations in the Bergmann astroglia observed in this study will be compared and contrasted to research previously reported. Also, the presence or absence of growth cones, necrotic debris and whorls that inhabit areas of the external differentiating, molecular and internal granule cell layers at some stage in development of the cerebellar cortex, will be compared and contrasted to structures observed within control and MAM-injected mice.

LITERATURE REVIEW

In early studies on the carcinogenicity of cycad meal and cycasin (methylazoxymethanol glucoside), Hirano and Shibuya (1967) accidentally found that mice injected with cycasin (0.5 mg/gm body weight) at day zero exhibited physical signs due to a neurological deficit. They reported that the mortality rate in mice injected with cycasin was 15% by postnatal days 5-15, and 33% by postnatal days 20-33. Eighty percent of the mice showed ataxia and posterior paralysis by postnatal day 20, and these signs were irreversible by postnatal day 33.

PHYSICAL EXAMINATION

In experiments to determine the effects of cycasin or MAM on neonatal Swiss albino mice, many physical changes were observed (Jones, 1971). These experiments showed that there was a delay in the appearance of fur or the opening of the eyes by a few days, even though the climbing abilities or righting abilities were not impaired (Jones, 1971; Jones, et al., 1972a; Jones, et al., 1973). Jones, et al. (1973) performed sequential neurological evaluations through 25 days of age on cycasin-injected mice. Sixty percent of the treated mice exhibited some aberrant physical, motor or postural changes sometime during their initial 25

postnatal days, with only thirty percent remaining symptomatic at 25 days of age. By ninety days, none of the less severely affected cycasin treated mice showed symptoms, indicating an apparent recovery from their previous neurological deficits.

Lane (1964) described Weaver mutant mice which exhibited clinical neurological signs similar to those observed in cycasin and MAM-treated mice (Jones, et al., 1972a). At about eight to ten days the first clinical neurological signs in the Weaver were exhibited with the instability of gait. After several steps the animal would fall to one side. At the second or third week the incoordination abated slightly with more stable locomotion. The adults appeared to compensate for their neurological defect by lowering their bodies to the surface they were upon, and widening their stance in order to maintain an upright position. Their limbs were poorly coordinated, especially the hind limbs. They also exhibited a fine rapid tremor of the extremities and trunk that was superimposed upon their slow swaying movements. The neurological signs in the Weaver do not appear to be worsened with age (Lane, 1964).

Staggerer mice, another neurological mutant, exhibits partial recovery from neurological deficits. These mice are physically smaller than normal mice during their first postnatal week, and exhibit unsteadiness when attempting to

walk. This unsteadiness is even more apparent during the second and third weeks, with the mice exhibiting a transient hyperextension of the limbs, and a reduction in activity and vigor which leads to ataxia associated with a slight tremor of the limbs. In the adult stage, Staggerer mice are physically smaller and less active, with poor self-grooming habits, but their tremor appears to abate (Sax, Hirano and Shofer, 1968).

A tendency towards partial recovery from cerebellar deficits has also been observed in rats irradiated during the first postnatal days (Altman, et al., 1971; Anderson and Altman, 1972), in acute azide poisoning of monkeys (Mettler and Sax, 1972), and in hemicerebellectomized rats (Smith, Parks, and Lynch, 1974). A theory for the reduction of cerebellar deficits suggests that the recovery is due to the great plasticity in the neocortex. This plasticity allows for the formation of new or altered synaptic contacts on the presumably remaining pathways, thereby compensating for partial cerebellar damage (Altman, et al., 1971; Smith, et al., 1974).

MACROSCOPIC EXAMINATION

The definitive histologic changes seen in the cerebellums of MAM-injected mice consisted of destruction within the external differentiating cell layer (Jones, et al., 1972a). This destruction caused a concomitant decrease in the foliation as observed in midsagittal sections of the

cerebellum (Chanda, et al., 1973; Woodward, et al., 1975). Woodward, et al. (1975) planimetrically measured the sagittal sections of the vermis in rats at varying postnatal ages after injecting them with MAM (10 mg/Kg body weight) for four consecutive postnatal days. At day four, sagittal sections of the cerebellum were only 12% less in size than those of the control. At day seven, there was a 35% decrease in the MAM-injected rat sagittal vermis areas. At day 14, the reduction was diminished to 29%.

Reduction in midsagittal sections of the vermis has also been reported in various animals due to: a virus infection with feline panleukopenia (Herndon, et al., 1971; Llinas, et al., 1972; Margolis and Kilham, 1970); genetic defects in Weaver mice (Hirano and Dembitzer, 1975; Rakic and Sidman, 1973b, 1973c); Staggerer mice (Hirano and Dembitzer, 1975); Lurcher mice (Caddy and Biscoe, 1975); x-irradiation in rats (Altman and Anderson, 1971, 1972; Anderson and Altman, 1972; Altman, et al., 1971); inhalation of ethanol (Bauer-Moffet and Altman, 1975); and hyperthyroidism in rats (Lauder, Altman and Krebs, 1974). A 26% midsagittal vermis reduction has been observed within rats chronically subjected to high levels of ethanol (Bauer-Moffett and Altman, 1975). Of the genetic mutants, the heterozygous Weaver (+/wv) has shown a 5-10% midsagittal vermis reduction by the fourth postnatal day (Rakic and Sidman, 1973b), which increased to 20% at postnatal day 21

(Rakic and Sidman, 1973c). The homozygous Weaver (wv/wv) has concurrently shown a 70% reduction in size by postnatal day 21. The Lurcher mouse midsagittal vermis reduction has not been reported; but, published line drawings of the vermis show a size reduction similar to that observed within the homozygous Weaver. Sixteen day kittens, irradiated (200r) during the first two postnatal weeks, have exhibited up to a 58.5% midsagittal reduction in the size of the cerebellar ansiform lobule. The estimated maximal reduction of granule cells was 64% with 400r, while the same dosage destroyed very few Purkinje cells (Altman, Anderson and Wright, 1967). This concurs with the previously discussed studies showing that most of the reduction has been due to granule cell loss.

Purkinje cells

1. Disorientation of Purkinje cell somata

The previously described pathological processes that reduce midsagittal vermis areas, subsequently dislocate Purkinje cell somata which come to lie within the molecular and internal granule cell layers (Altman, et al., 1971; Anderson and Altman, 1972; Herndon, et al., 1971, Hirano and Dembitzer, 1975; Rakic and Sidman, 1973b, 1973c; Sax, et al., 1968).

Two theories have arisen that describe the dislocation of the Purkinje cell somata. In the first theory, Woodward, et al. (1975) proposed that MAM administered to newborn

mice causes reduction in the number of external differentiating cells, which slows the production of internal granule cells. The decreased cell production delays the "folial expansion" that is essential in providing sufficient area for the development of a normal Purkinje cell layer. A second theory suggests that a glial reaction and rapid "astrocyte swelling", in response to external differentiating and internal granule cell degeneration and necrosis, cause the misalignment and disorientation of Purkinje cell somata (Jones and Gardner, 1976).

2. Purkinje cell apical pole orientation

Altman and Anderson (1972) hypothesized that when the external differentiating cells and internal granule cells are destroyed by irradiation, the Purkinje cell changes seen are due to the absence of the interneurons and are not due to the direct damage produced by the radiation. With the destruction of the external differentiating cell layer the apical poles of the Purkinje cell somata which normally point towards the surface become randomly oriented. Altman and Anderson (1972) observed that the growth of the apical pole of the Purkinje cell "is an autonomous event, while the normal orientation of this growing structure depends on the presence and location of the external differentiating cell layer."

With the autonomous growth, the random orientation of the Purkinje cell, primary dendrites, somata, and the

unusual shapes of the arborizing dendrites can be explained (Altman and Anderson, 1972; Woodward, et al., 1975).

3. Multiple and massive primary dendrites

Woodward, et al. (1975) suggested a hypothesis for the formation of multiple primary dendrites. In the absence of parallel fibers due to the granule cell destruction, dendritic growth may spread from several early Purkinje somatic projections. With the late appearance of large numbers of parallel fibers in treated animals, one or more Purkinje cell processes may develop into a dendrite with secondary and tertiary branches. If a particular dendrite does not reach a group of parallel fibers, multiple primary dendrites continue to grow and become progressively more difficult to reabsorb the larger they become.

In the absence of a favorable environment, the immature growing process of the dendrites (filopodia) will attempt to reach one. After growing farther from the soma into a more suitable environment, the dendrite will then mature into secondary and tertiary branches and branchlets with spines (Woodward, et al., 1975). The same authors illustrated the random orientation of dendrites that in some cases become abnormally oriented perpendicular to (rather than within) the sagittal plane. After the initial cellular destruction by MAM or x-ray, the few remaining external differentiating cells begin their regeneration.

The reorientation appears to be towards the regenerating cells (Altman and Anderson, 1972; Woodward, et al., 1975).

After irradiation of the cerebellum, Altman and Anderson (1972) observed many thick blunt spines on massive primary dendrites forming synapses with climbing and mossy fibers and "pseudosynapses" with glia cells. They attributed the lack of spiny branchlets due to the paucity of granule cells and their parallel fibers projecting into the molecular layer. They suggested that spine formation is dependent upon the presence of parallel fibers and is not an autonomous process.

Golgi epithelial (Bergmann) astroglia

As Bergmann astroglia develop, they send vertical ascending processes from the Bergmann fibers straight through the neuropil of the molecular layer toward the pial surface. During further differentiation, the vertical processes develop "excrescences" 1 - 2 um long with drumstick terminal enlargements in close proximity to passing parallel fibers (Palay and Chan-Palay, 1974). Each expansion comprises a sheath which encapsulates a Purkinje cell dendritic spine except for the area of its synaptic attachment with a parallel fiber (Rakic, 1971).

Cerebellar abnormalities seen in Weaver mice may be associated with a reduced rate of granule cell migration (Rezai and Yoon, 1972). Rakic and Sidman (1973a, 1973b) proposed that the defective neuronal migration is secondary

to maldevelopment of Bergmann glia. Bignami and Dahl (1974) indicated that there is "an abnormality on the surface of the Bergmann fibers, preventing 'recognition' from migrating neurons, rather than the physical absence of these fibers serving as guidelines for neurons migrating through the molecular layer."

External differentiating plus internal granule cell reduction and regeneration

Methylazoxymethanol glucoside (cycasin) and methylazoxymethanol acetate (MAM) have been shown to selectively destroy dividing microneurons when injected into mice, rats or hamsters (Calvet, Drian and Privat, 1974; Chanda, et al., 1973; Chanda, Woodward, and Griffin, 1975; Hirano, et al., 1972; Hirano and Jones, 1972; Jones, et al., 1973; Jones, Sweeley, and Yang, 1972b; Jones and Gardner, 1976; Shimada and Langman, 1970; Woodward, et al., 1975).

In developmental and comparative light microscopic studies Jones, et al. (1972a, 1973) injected Swiss albino mice with cycasin (0.5 mg/gm body weight), MAM (0.05 ul/gm body weight) or physiological saline within the first 24 hours after birth. As early as six hours, cellular necrosis was evident within the external differentiating cell layer in MAM-injected mice. Cycasin and MAM-injected mice both exhibited extensive necrosis in the external differentiating cell layer by three days postinjection. By the fifth post-injection day both the external differentiating and internal

granule cell layers were markedly diminished, while the misaligned Purkinje cells were scattered in the molecular and internal granule cell layers.

The regeneration has also been described in MAM-treated hamsters (Shimada and Langman, 1970) and is similar to the cytological events described after x-irradiation (Altman, Anderson and Wright, 1969). Chanda, et al. (1973) confirmed that regeneration had indeed taken place, by noting an increasing amount of DNA, RNA and protein during the recovery phase. They raised the question about the degree of function associated with regeneration.

SYNAPTOGENESIS

Synapse formation begins when transient contacts of growing axonal processes stop their migration and form permanent synaptic sites, composed of a synaptic cleft which joins the pre- and postsynaptic elements (Cotman and Banker, 1974). What is the structure of a mature axodendritic synapse? What are the ultrastructural features of parallel fiber-Purkinje cell dendritic spine synapses? How is the synaptic complex formed? What alterations of the synaptic complex are observed in pathological conditions?

Structure of a mature axodendritic synapse

A mature axodendritic synapse is the site for transmission of impulses from an axon to a dendrite. The synapse consists of three structures: the synaptic cleft, a pre-, and post-synaptic element. The pre- and postsynaptic

elements are joined by a synaptic cleft approximately 160 Å in width, with intercleft lines on each side of the cleft (60 Å in width), resulting in a gap from pre- to postsynaptic elements of approximately 225 to 300 Å (Akert, et al., 1972). The cleft contains either fine, or smaller tufted densities, tipped with a knob that sometimes extends to the middle of the cleft but not entirely across it, or both of these structures (Gray, 1966).

The presynaptic element is a dilated structure that contains several mitochondria and synaptic vesicles, 300 to 500 Å in diameter (Gray and Guillery, 1966). These vesicles aggregate near the presynaptic thickening, which contains regularly spaced dense projections that appear to make up a lattice structure. The postsynaptic element consists of an electron dense thickening that may extend up to 200-500 Å into the postsynaptic cytoplasm (Akert, et al., 1972; Gray and Guillery, 1966; Cotman and Banker, 1974).

Gray (1959) described two types of synapses and distinguished them according to the width of the postsynaptic density. Type I is an asymmetrical synapse (like those observed at parallel fiber-Purkinje cell dendritic spine junctions) with a postsynaptic density approximately 200-500 Å in width. The symmetrical Gray type II synapse is similar to the type I, except that the postsynaptic density is 100-200 Å in width.

Ultrastructure of Purkinje cells, granule cells, and their processes

The mature Purkinje cell soma is 20-40 um in diameter. Its cytoplasm is rich in granular and agranular endoplasmic reticulum, hypolemmal cisternae (which are about 600 Å beneath the plasmalemma and parallel to it), Golgi apparatus, lysosomes, mitochondria, neurotubules, and neurofilaments. The dendritic tree arises in one to four primary dendritic trunks from the apical pole of the cell and passes in a sagittal plane at right angles to the cerebellar folial surface. The purkinje dendritic tree contains primary, secondary (1-7 um in diameter at some points of bifurcation), and tertiary dendrites and branchlets (0.5-2 um in diameter). Numerous spines project from the tertiary dendrites and branchlets. At its initial segment, the Purkinje cell axon looks like an elongated part of the cell body because it contains not only neurofilaments, but also endoplasmic reticulum, and numerous ribosomes that are usually absent in an axon. As the axon passes toward the medullary portion of the cerebellum, it sends off collaterals to the Lugaro cells, other Purkinje cells, Golgi II cells, and granule cells (Herndon, 1964; Palay and Chan-Palay, 1974).

Granule cells that have completed their migration into the inner granule cell layer have perikarya about 7-10 um in diameter in mice and rats. A large nucleus is

surrounded by a thin rim of cytoplasm (0.1 to 0.3 um thick). Chromatin granules form clumps which are scattered through the nucleoplasm. The thin rim of cytoplasm contains: free ribosomes, a few mitochondria (0.1-0.3 by 2-4 um), membranes of endoplasmic reticulum (0.2-2.0 um in diameter), Golgi apparatus (on one side of the cell where there is an expansion of cytoplasm), and no Nissl substance. The unmyelinated ascending axon (0.1-0.3 um in diameter) of the granule cell passes upward to the molecular layer where it bifurcates to become the parallel fibers (0.1-0.2 um in diameter). At 1.7 to 2.5 um intervals along the parallel fibers there are varicosities (0.5-1.0 um in diameter) which contain a loose collection of round synaptic vesicles. Normally, these varicosities articulate with Purkinje cell dendritic spines, basket cells, stellate, or Golgi cell dendrites (Gray, 1961; Herndon, 1964; Palay and Chan-Palay, 1974). Parallel fibers average 0.6 mm in length in the mouse and synapse with an average of 29 Purkinje dendritic spines. Two hundred thousand to three hundred thousand parallel fibers course through each Purkinje cell arborization. The granule cell dendrites, located in the internal granule cell layer, are rather short, and synapse with the mossy as well as Golgi II axons and dendrites (Palay and Chan-Palay, 1974).

The junction between the parallel fiber and Purkinje cell dendritic spines is a Gray's type I asymmetrical

synapse. The synaptic cleft is widened to about 300 Å, with occasionally occurring fine filaments crossing the synaptic cleft (Palay and Chan-Palay, 1974). The presynaptic parallel fiber varicosities that synapse with the Purkinje cell dendritic spines contain synaptic vesicles (240-440 Å in diameter). These synaptic vesicles aggregate among tufted densities interwoven filaments (50 Å in diameter), that extend from the axolemma. Mitochondria and microtubles are also found within the presynaptic varicosities.

The postsynaptic elements are composed of spines attached to dendritic branchlets. They are 1.0-2.0 um long, with bulbous heads 0.4-0.6 um across on a stalk 0.2-0.3 um but they occasionally contain cisternae and tubules among the fine filamentous matrix. The postsynaptic density (the postsynaptic element) is an electron dense structure that may extend up to 440 Å into the postsynaptic cytoplasm (Palay and Chan-Palay, 1974). In adult animals, Bergmann astroglial processes that normally surround Purkinje cell dendrites, also encompass parallel fiber-Purkinje cell dendritic spine synapses.

Synaptogenesis: development of parallel fiber-Purkinje cell contacts

Larramendi (1969) described parallel fiber-Purkinje cell dendritic spine synaptogenesis as taking place in stages in 14 day Swiss albino mice. In the first stage,

immature parallel fibers and ascending axons from the granule cells appear thicker in diameter than mature parallel fibers. They are densely packed without any intervening glia, contain numerous microtubules, and lack synaptic enlargements or swellings. As parallel fibers and Bergmann astroglia mature, glial processes associated with Purkinje cell dendrites expand to encompass nearby parallel fibers or axonal bundles. Numerous long, slender spines without membrane specializations, observed protruding from the Purkinje cell dendrites, grow in between the parallel fibers. After parallel fiber-Purkinje cell dendritic spines contact each other, membrane specializations form and a few synaptic vesicles adhere to the presynaptic site, barely enlarging the parallel fiber.

Stage two, commences when the Purkinje cell dendritic spines appear to shorten and the well developed head slightly invaginates into the parallel fiber varicosity. The varicosity now contains many synaptic vesicles and a few mitochondria (Larramendi, 1969). Larramendi (1969) assumed that contact between these pre- and postsynaptic elements preceded the appearance of synaptic vesicles and pre- and postsynaptic membrane densities.

Growth cones

The early formation of "growth cones", suggested by del Cerro and Snider (1968) are recognized by a local accumulation of vesicles about 400-1100 Å in diameter in an

area of the neuroblast near the cell membranes. A protrusion of a short, thick process, containing numerous vesicles, precedes by elongation, with mitochondria and ribosomes moving into the proximal portion of the outgrowing process. Within the molecular layer, both the Purkinje cell dendrites and parallel fibers end in "terminal growth cones"; "subterminal growth cones" precede spine formation (del Cerro and Snider, 1972; Johnson and Armstrong, 1970). Both terminal and sub-terminal growth cones are present in the Purkinje cell dendrites at 9-12 days and persist until adulthood (del Cerro and Snider, 1968).

Naked Purkinje cell dendritic spine specializations

Since Larramendi's report, naked Purkinje cell dendritic spine specializations have been shown to differentiate in the absence of a parallel fiber presynaptic element. This phenomenon is seen in various models when parallel fiber reduction is secondarily produced by cycasin or MAM (Hirano, et al., 1972; Hirano and Jones, 1972; Jones, et al., 1972; Jones, et al., 1973), viral infection with feline panleukopenia (Herndon, et al., 1971; Llinas, et al., 1972); gene mutations (Hirano and Dembitzer, 1973, 1975; Sotelo, 1973, 1975); x-ray (Altman and Anderson, 1972, 1973); or tissue culture (Seil and Herndon, 1970; Kim, 1975). Each pathological process has a different mechanism, but they all eventually cause the destruction

of the external differentiating cell layer and secondary reduction of internal granule cells, thereby producing an agranular cerebellum. In this setting, postsynaptic sites on Purkinje cell dendritic spines appear to differentiate.

Rats treated on postnatal days one through four with MAM (10 mg/kg body weight) exhibited extensive destruction of external differentiating cells during the first four postnatal days (Chanda, et al., 1973). At postnatal day seven the cerebellum in the treated animals exhibited a reduced foliation. By postnatal day 14 the external differentiating cell layer had regenerated and become thicker than in controls. By postnatal day 21 the external differentiating cell layer was almost totally absent due to the inward migration of cells, like in the controls (Woodward, et al., 1975).

When cycasin (0.5 mg/gm body weight) and MAM (0.05 ul/gm body weight) were injected into zero day mice and examined 25 days postnatal, the molecular layer contained a significantly reduced parallel fiber population and a number of naked Purkinje cell dendritic spine specializations embedded in a matrix of astrocytic cytoplasm (Hirano, et al., 1972; Hirano and Jones, 1972; Jones, et al., 1973).

Cats and ferrets injected at birth with feline panleukopenia virus exhibited naked Purkinje cell dendritic spine specializations when sacrificed in adulthood. The virus primarily destroyed the external differentiating cell

layer and secondarily reduced this cell population. Deafferented Purkinje dendritic spines were then enveloped by hypertrophic glial cytoplasm of the Bergmann astrocytes (Herndon, et al., 1971).

Hirano and Dembitzer (1973) examined the Purkinje cell spines of the mutant mouse, Weaver. In this mutant, parallel fibers may fail to form due to a reduced rate in the granule cell migration (Rezai and Yoon, 1972). Rakic and Sidman (1973a, 1973b) proposed that defective neuronal migration is secondary to maldevelopment of Bergmann glia. Bignami and Dahl (1974) indicated that there is "an abnormality on the surface of the Bergmann fibers." This prevents the 'recognition' of migrating neurons, that use the fibers as guidelines during their migration through the molecular layer. Naked Purkinje cell dendritic spine specializations were clearly demonstrated in this genetic mutant (Hirano and Dembitzer, 1973).

Within another mutant, the Staggerer, the Purkinje cells are abnormal. Tertiary dendritic branches, branchlets and spines are missing. The normal target for parallel fibers, which occasionally form presynaptic grids (a normal presynaptic element with synaptic vesicles facing a Bergmann astroglial process) is thus eliminated. Secondary degeneration of granule cells occurs (Hirano and Dembitzer, 1975; Sotelo, 1973; Sotelo and Changeux, 1974). Some Purkinje cell dendritic spines on tertiary branches

and branchlets do appear at 23 postnatal days but were mostly absent by three months. Naked Purkinje cell dendritic spine specializations were seen only in 3 month mice (Hirano and Dembitzer, 1975).

Prolonged x-irradiation, like panleukopenia, cycasin, and MAM, destroys cerebellar granule cells in rats before migration (Altman, et al., 1967; Altman and Anderson, 1971, 1972; Anderson and Altman, 1972; Hopewell, 1974; Woodward, Hoffer and Altman, 1974). Purkinje cells still form their characteristic dendritic branching pattern and even form naked Purkinje cell dendritic spine specializations (Altman and Anderson, 1972, 1973).

Cultivation of rat and mouse cerebellums has resulted in the growth and development of various types of cerebellar neurons, including Purkinje and granule cells (Kim, 1975; Seil and Herndon, 1970). Kim (1975), Seil and Herndon (1970) have observed the concurrent development of naked Purkinje cell dendritic spine specializations. When rat cerebellums are cultivated in the presence of MAM, naked Purkinje cell dendritic spine specializations are produced in the almost total absence of any other cells (Calvet, et al., 1974).

These experiments are significant because they show that naked Purkinje cell dendritic spine specializations form autonomously and in the absence of parallel fibers. The capacity to initiate production of these specializations may therefore be intrinsic to the postsynaptic cell.

The appearance of naked Purkinje cell dendritic spine postsynaptic densities implies either degeneration of presynaptic elements after the formation of normal synaptic contacts, or the formation of these dendritic spine specializations by some other mechanism. Kim (1975) relates that if the first hypothesis is to be substantiated, degenerating presynaptic terminals should be demonstrated. If another mechanism is responsible for the development of these structures, degenerating presynaptic terminals should not be demonstrated. One of three possible mechanisms might explain the formation of Purkinje cell dendritic spine specializations in the absence of a presynaptic element. The first mechanism is the endowment of Purkinje cells with the ability to form dendritic spine specializations independent of presynaptic input (de novo formation, Altman and Anderson, 1972). A second mechanism would involve the formation of dendritic spine specializations after the stimulation of synaptic contacts on a Purkinje cell by afferents from climbing fibers or contacts other than granule cell parallel fibers (Hamori, 1973; Sotelo, et al., 1975). The third mechanism would involve the induction of Purkinje cell dendritic spine specializations by stimulation of a small number of synaptic contacts between parallel fibers and Purkinje cell dendritic spines (Hirano and Dembitzer, 1974).

Durability of naked Purkinje cell dendritic spine specializations

Naked Purkinje cell dendritic spine specializations have been reported to be durable structures remaining intact for long periods of time (up to a year) (Hamori, 1968, 1973; Herndon, 1968; Herndon, et al., 1971; Hirano and Dembitzer, 1975; Sotelo, 1973, 1975).

A relatively recent theory proposes that the naked Purkinje cell dendritic spine specializations on tertiary branches and branchlets are maintained by climbing fiber contacts upon the primary and secondary Purkinje cell dendrites (Hamori, 1973). As a result, Sotelo (1975) in contrast to Hamori, suggests that naked Purkinje cell dendritic spine specializations are autonomous in their appearance and stability, which supports the theory of de novo formation and independent maintenance of naked spine specializations.

Necrotic debris

Ultrastructurally, cellular necrosis within the external differentiating cell layer has been observed as early as six hours following MAM-administration with extensive necrosis present three days postinjection. By the fifth postinjection day the external differentiating and internal granule cell layers have been shown to be markedly diminished with necrosis not evident after five days postnatal in MAM or cycasin-injected mice (Jones, et al., 1972a, 1973). Jones and Brownson (1969) observed that necrotic

debris in the normal differentiating hippocampus was surrounded by a pale watery cytoplasm similar to the appearance of astrocytes. This phenomenon was also observed after thiophen necrosis by Herndon (1968).

Cell degeneration and necrosis has been observed within Golgi cells from normal 10 day mice (Larramendi, 1969) and within normal fetal rat central nervous system. These may be normal processes for the removal of a vestigial organ or cells (Maruyama and D'Agostino, 1967).

A host of methods previously described has been used for the destruction of cells of the cerebellar external differentiating or internal granular cell layers. Necrosis has been a prominent feature at some point in the process followed by the removal of cellular debris. This probably is accomplished by phagocytic cells which migrate from the blood vessels. However, astrocytes assume a phagocytic role, too (Herndon, 1968; Jones et al., 1973).

Whorls

Membranous whorls composed of smooth concentric membranes were occasionally observed within astrocytes (Palay and Chan-Palay, 1974; Sotelo and Palay, 1971; Hirano, et al., 1972). They were encountered in both foot processes and bulbous terminals of Bergmann astroglia as well as within Bergmann astroglial fibers. The concentric lamellated whorls composed of collapsed cisternae appeared to be derived from endoplasmic reticulum and mitochondria

(Palay and Chan-Palay, 1974; Sotelo and Palay, 1971). They resembled concentric laminar membranes observed in axon terminals. Smooth membranes have been shown to have the capability of producing intracellular concentric whorls and have been shown to occur also in a variety of non-neural tissues (Sotelo and Palay, 1971). They suggest that the overproduction of smooth membranes is characteristic of developing, growing or regenerating axons. In contrast, spirals without any type of cistern separating the lamellar membranes have also been observed within saline and MAM-injected mice. Chan-Palay (1973) and Larramendi (del Cerro and Snider, 1969) believe that this is a fixation artifact, while del Cerro and Snider (1969) showed similar structures in Purkinje cell dendrites and suggested the production was due to a toxic drug effect.

METHYLAZOXYMETHANOL ACETATE (MAM)

The initial studies of methylazoxymethanol glucoside (cycasin) were due to the interest in the toxicity appearing in sheep and cattle grazing on the cycad during long, hot, dry spells in Guam (Jones, et al., 1973). The resulting experiments showed that a fatal neurological disorder occurred in cattle following ingestion of cycad leaves. Neurological diseases commonly observed in natives and their use of cycad flour as a food supplement, raised the question of associated central nervous system toxicity (Jones, et al., 1973; Whiting, 1963). Subsequent studies

failed to reveal an histopathologic basis for the neurological disorders in cattle or to establish a definite connection with human neurological disease. Cycasin and its derivative, methylazoxymethanol acetate (MAM), were found to be hepatotoxic (Ganote and Rosenthal, 1968; Zedeck, et al., 1970), teratogenic (Spatz, Dougherty and Smith, 1967) carcinogenic (Hirano, 1969), and neurotoxic (Hirono and Shibuya, 1967) when administered to a host of animals. Jones and other investigators have shown that the neurotoxic effects are confined to dividing cells in the central nervous system (Jones and Gardner, 1976).

The glucoside or the acetate of methylazoxymethanol acts by methylating the 7 position of guanine in the brain nucleotides, causing disruption of DNA and RNA function (Chanda, et al., 1975; Jones, et al., 1973; Matsumoto and Higa, 1966; Nagata and Matsumoto, 1969; Shank and Magee, 1967). MAM appears to have little neurotoxic effects on mature differentiated cells within the central nervous system since there are no cerebellar behavioral changes nor loss in cerebellar DNA if MAM-injections are given after 21 days of age in rats (Chanda, et al., 1975). Dividing cells are most susceptible to damage by MAM (Chanda, et al., 1975; Jones, et al., 1973).

MATERIALS AND METHODS

Newborn Swiss albino mice, Webster strain (obtained from Spartan Research Animals Inc., Haslett, Michigan) were selected randomly from six litters (which had been reduced to 10 pups per litter) examined, weighed, marked for identification and injected with methylazoxymethanol acetate (MAM) (0.05 ul/gm body weight) or saline (0.05 ul/gm body weight) (Appendix A). Both (saline and MAM-injected) groups were housed in plastic shoebox cages containing pinechips. Controlled room temperature, humidity and a standard light-dark cycle were maintained. All mice in each group were sacrificed at 10 days of age after they were again weighed. Specific factors were assessed and recorded after physical examination (Appendix A). Eight mice from each group (the number of MAM-treated mice remaining alive at 10 days and the saline or MAM-injected group) were anesthetized with Nembutal (sodium pentobarbital, 0.05 mg/gm body weight). After thoracotomy and exposure of the heart, heparin (300 units/animal) and sodium nitrite (0.01 ml/gm body weight of a 1% solution) were injected into the left ventricle. The mice were then perfused (Appendix A) with 1% glutaraldehyde and 0.5% paraformaldehyde in a 0.12 M standard phosphate buffer containing 0.02 mM $CaCl_2$ to establish a pH of 7.65 at 520 mOsM (using a technique modified from Palay and Chan-Palay, 1974).

Rapid Golgi impregnation: After perfusion for 20 - 30 minutes, three cerebellums from each group (saline or MAM-injected) were removed and immersed in a 2.33% potassium dichromate and 0.19% osmium tetroxide solution for ten days followed by one day in 0.75% silver nitrate at room temperature (Rapid Golgi technique from Palay and Chan-Palay, 1974). They were then embedded in routine fashion in paraffin, sectioned at 75 - 125 um on a Sorval TC-2 tissue sectioner and mounted on slides. Photomicrographs of the Golgi sections and all other light microscopy were taken on a Zeiss Photomicroscope II. A morphometric evaluation of sagittal sections of the vermis was made with the use of a Bausch and Lomb Microprojector and a Hartkop Counting Chamber (Appendix A), (modified from a Method according to Weibel, Kistler and Scherle, 1966).

The remaining five mice from each group (saline or MAM-injected) were perfused for 20 - 30 minutes. The skulls were opened and the heads placed in fresh fixative at 4°C overnight. The following morning one-half of the cerebellum was postfixed in 10% buffered formalin, embedded in paraffin, sectioned, and mounted slides stained in routine fashion with Harris hematoxylin-eosin (Luna, 1968; Sheehan and Hrapchak, 1973) or Luxol fast blue-cresyl violet (Luna, 1968). The vermis from the second half of each cerebellum was postfixed for two hours in 2% osmium tetroxide in a 0.12 M standard phosphate buffer with a 3.5% dextrose, and

then rinsed in a 0.1 M sodium acetate solution. They were then stained en-bloc with 0.5% uranyl acetate for 30 minutes at 4°C, dehydrated through graded alcohols, and embedded in Epon-araldite (modified from Palay and Chan-Palay, 1974). One micron thick sections were stained with 1% toluidine blue for study by light microscopy. Thin sections (600 - 800 Å) were stained with lead citrate 1 - 2 minutes and uranyl acetate for 30 - 90 minutes according to the methods of Reynolds (1963), Venable and Coggeshall (1965).

Ultrastructurally, the Purkinje cell dendrites, granule cell parallel fibers and their synapses were qualitatively assessed for the presence or absence of certain structures with the use of a Philips 201 electron microscope. The structures assessed were: naked Purkinje cell dendritic spines with a postsynaptic thickening, Purkinje cell dendritic spines, normal synaptic cleft of 200 - 300 Å within a normal parallel fiber-Purkinje cell dendritic spine synapse, naked presynaptic varicosities, presynaptic terminals (varicosities on parallel fibers), growth cones, microtubules and postjunctional dense bodies (Appendix A, Electron Microscopic Data Sheet). The measurement of structures in the micrographs was accomplished with the use of a Hartkop Electron Microscopic Measurement Nomograph (Appendix A).

Chart 1. FLOW DIAGRAM FOR DETERMINING THE PRESENCE OF NAKED PURKINJE CELL DENDRITIC SPINES AND OTHER PATHOLOGICAL CHANGES IN 10 DAY SALINE AND METHYLAZOXYMETHANOL-INJECTED SWISS ALBINO MICE.

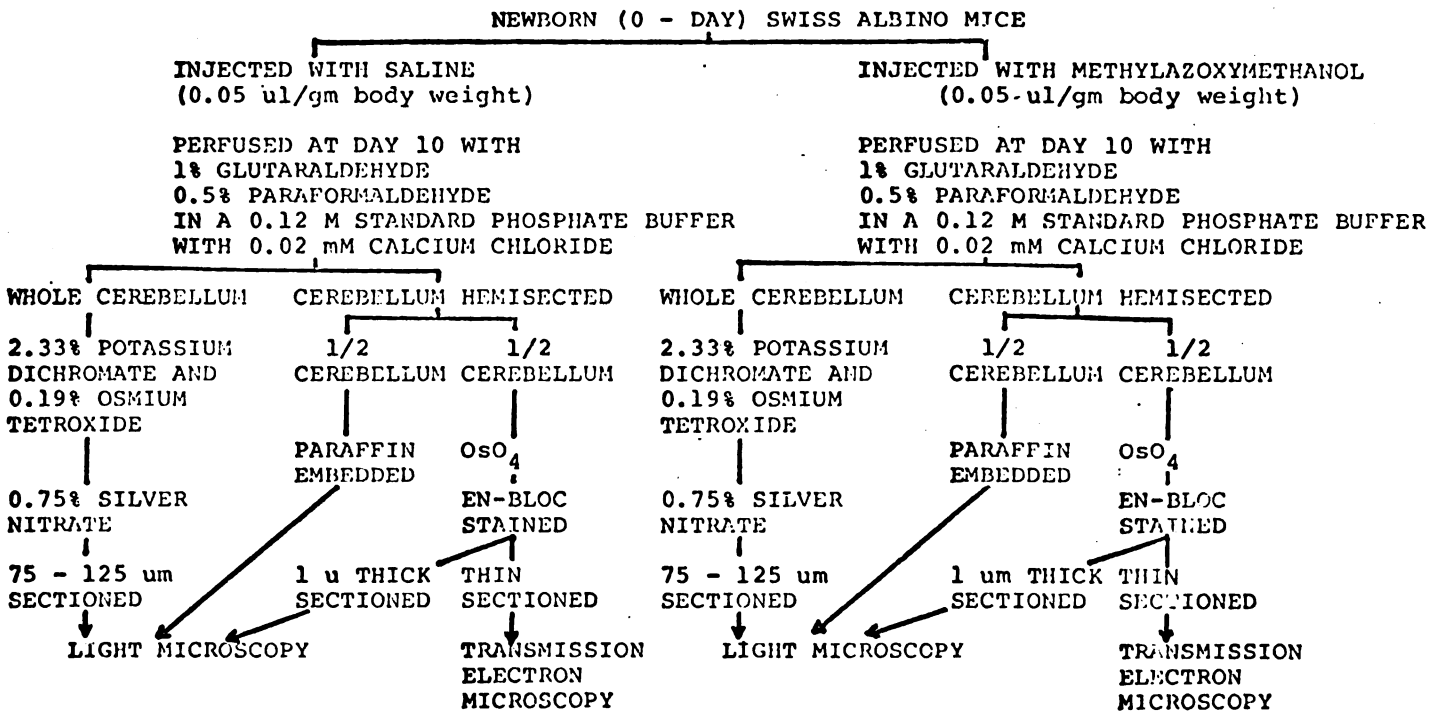

RESULTS

PHYSICAL EXAMINATION

At day zero the weights of the saline-injected and the MAM-injected animals were not significantly different. The average body weight was 1.7 grams at day zero. Prior to the perfusion at day 10, the average weight of the saline-injected animals was 6.19 $\pm$ 0.58 grams while that of the MAM-injected mice was 5.22 $\pm$ 0.84 grams (a difference which is significant at the 0.005 level). The general activity, climbing abilities and righting abilities were equal in both groups (saline and MAM-injected) at day zero and 10 as previously reported (Grondin *et al.*, 1975; Jones *et al.*, 1972a). Both groups of mice also exhibited a tremor of the head and body at days zero and 10. At day zero both groups of mice (saline and MAM-injected) were hairless. At day 10 however, all of the saline-injected mice had smooth white hair, while only one of the six mice in the MAM-injected group exhibited hair growth. At day zero all of the mice positioned their legs to the side, which is normal for this age group. At day 10 however, three out of eight saline-injected mice positioned their feet flat with legs tucked underneath, which is the normal position for adults, while the other five positioned their legs laterally to the side. The three 10 day saline-injected mice with feet in the normal position appeared more mature than the other saline-injected mice. All of the 10 day MAM-injected mice

positioned their legs to the side and appeared more immature (Figure 1). The difference between the MAM- and saline-injected mice was significant at the 0.05 level.

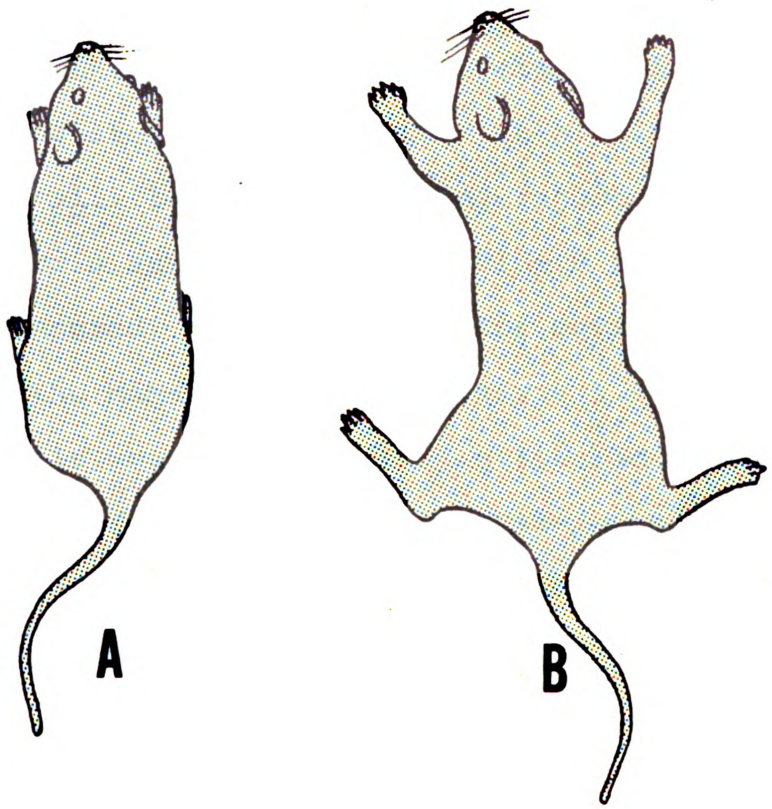

Figure 1. With the mice in the prone position, figure 1A illustrates the normal position of the legs in the adult and the mature 10 day mouse. Figure 1B illustrates the lateral position of the legs in the newborn and immature 10 day mouse.

MACROSCOPIC EXAMINATION OF THE CEREBELLAR VERMIS

Gross examination of the cerebellum and brain revealed a reduction in cerebellar size in all MAM-injected animals in contrast to the controls (Fig. 2). The reduction in size was confirmed by measurement of the surface area of sagittal sections of the vermis which was similar to that consistently demonstrated in previous experiments (Jones, et al., 1973). The saline-injected animals had an average vermis surface area of 4.91 ± 0.52 mm^2 (five animals measured). Sagittal section surface area of the vermis in the MAM-injected animals was 1.98 ± 0.51 mm^2 in eight animals measured. This is a 60% reduction in the surface area of the vermis in the MAM-injected animals when compared to the saline control animals and is significant at the 0.005 level (Chart 2).

Figure 2. A comparison of areas and shapes of sagittal sections through the cerebellar vermis of eight 10 day mice injected with MAM (T43-10, T61-4, T61-5, T63-1, T63-2, T63-4, T65-4, T65-8) and five 10 day mice injected with saline (T32-1, T32-2, T32-5, T60-1, T62-7) shows significant reduction in surface areas secondary to MAM-induced differentiating cell loss. MAM-injected animal T43-10 and saline-injected animals T32-1, T32-2, and T32-5 were from a group of 10 day mice previously perfused, and were not studied on the ultrastructural level. They were injected and perfused in the same manner as litters T61 - T66.

Figure 2.

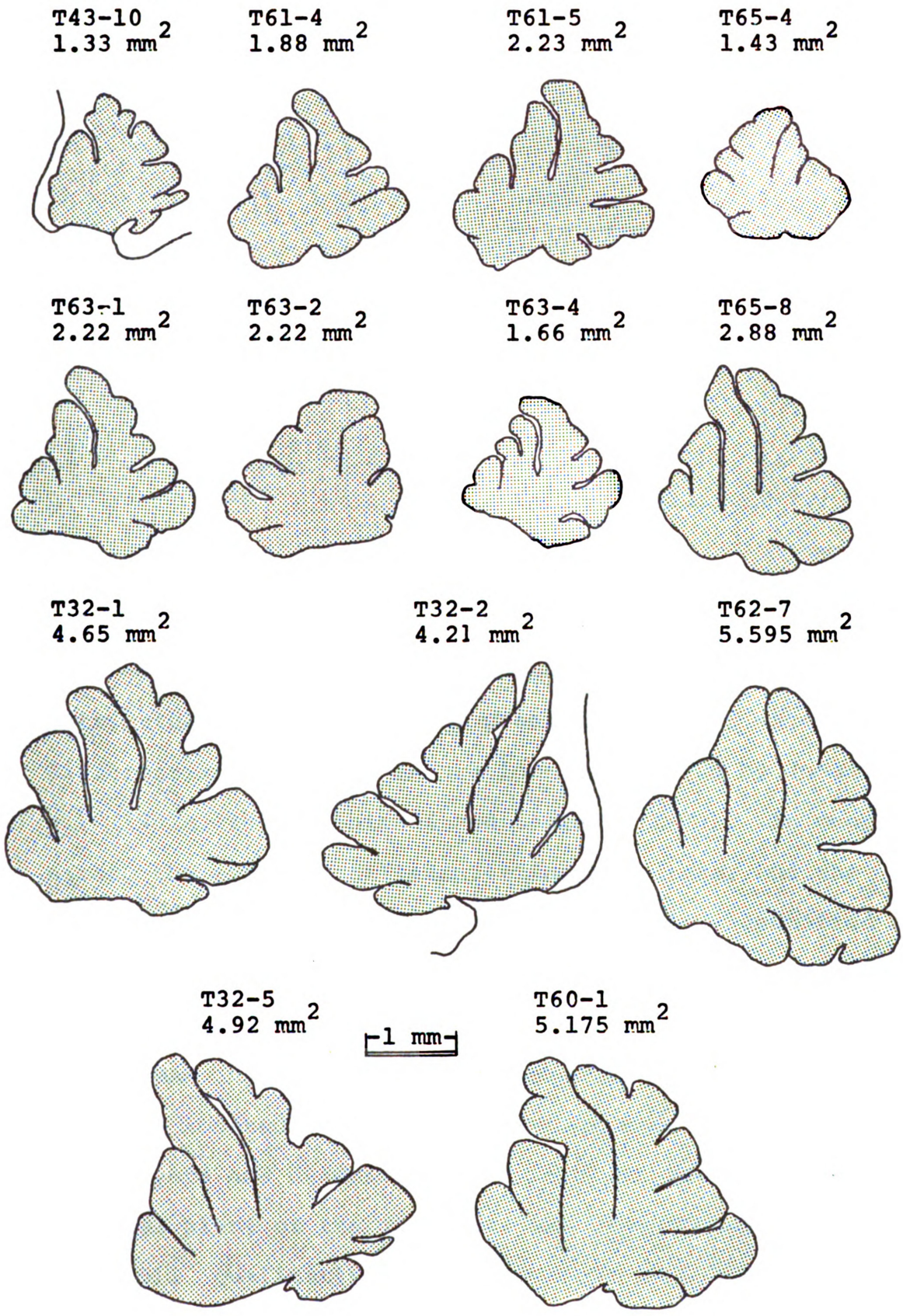
T43-10
1.33 mm2
T61-4
1.88 mm2
T61-5
2.23 mm2
T65-4
1.43 mm2
T63-1
2.22 mm2
T63-2
2.22 mm2
T63-4
1.66 mm2
T65-8
2.88 mm2
T32-1
4.65 mm2
T32-2
4.21 mm2
T62-7
5.595 mm2
T32-5
4.92 mm2
1 mm
T60-1
5.175 mm2

Chart 2.

	SALINE	MAM
Average sagittal surface area	4.91 mm^2	1.98 mm^2
Standard Deviation	0.52	0.51
Reduction of sagittal surface area in MAM mice		60%

LIGHT MICROSCOPIC EXAMINATION OF CEREBELLUM

The 60% reduction at 10 days of age in the surface area of the vermis in MAM-injected animals could be attributed to the paucity of granule cells and external differentiating cells, as previously reported by Jones, et al. (1972a, 1973), Shimada and Langman (1970). In many areas, the external differentiating cell layer and the granule cell layer could not be specifically identified and the putative molecular layer was occupied by dislocated Purkinje cells (Figs. 3 and 4). In many areas of the vermis, in the MAM-injected mice, the Purkinje cell somata were randomly located within the molecular and internal granule cell layers and dendritic trees were not visible in the sagittal plane of the molecular and granule cell layers (Fig. 5). Qualitatively, the Purkinje cell somata appeared

to be the same size in both groups (saline or MAM-injected) at 10 days of age. The apical poles (the initial portions of the primary dendrites) of the Purkinje cells in the MAM-injected mice were randomly oriented with their dendritic branches assuming a great variety of shapes. When the Purkinje cell somata are located near the surface, the dendritic branches may resemble a "weeping willow" with the dendrites deflected downward after reaching the surface. If the apical pole is oriented sideways, the primary dendrite may course parallel to the pial-glial surface and others with the apical pole oriented away from the pial-glial membrane may send their primary dendrites into the inner granule cell layer (Fig. 6) (Altman and Anderson, 1971, 1972; Mouren-Mathieu and Colonnier, 1969; Woodward, et al., 1975). Golgi impregnation studies revealed several alterations of the Purkinje cells which had not been observed in previously published MAM-injected animal studies (Jones, 1971, 1972a; Woodward, et al., 1975). There were many massive processes from each cell body which had characteristics of primary dendrites, but were larger in diameter (Figs. 7B and 8). The secondary and tertiary dendritic branches and branchlets were fewer in number. The dendrites were distributed in three dimensions, in contrast to the two dimensional orientation in the normal cerebellum (Fig. 7A). The dendrites were 30 - 40 um in length compared to the 60 - 80 um seen in the normal 10 day

Swiss albino mouse. Due to the reduced number of secondary and tertiary branches and branchlets in the MAM-injected mice, each dendritic arborization contained a reduced number of spines as illustrated in Golgi impregnated sections (Fig. 7).

The cells in the external differentiating cell layer that are destined to become granule, basket and stellate cells were almost totally absent or severely diminished in many cerebellar folia of MAM-injected mice. Within many lobules of the MAM-injected mouse cerebellum there appeared to be fewer granule cells located in the granule cell layer than in the normal cerebellum (Figs. 3, 4, 5, 6). All of the differentiated granule cells (control and MAM-injected) appear to be the same general size (7 - 10 um) in diameter.

In the MAM-injected mice the lateral processes with warty excrescences of the Golgi epithelial cells were either greatly reduced in number or virtually absent (Figs. 9B and 9C). In the MAM-injected mice the lengths of the vertical processes also appear to be reduced and the Golgi epithelial (Bergmann) cell somata were thus located nearer to the pial-glial membrane (Figs. 9B and 9C) when compared to normal (Fig. 9A). Engulfment of necrotic cellular debris by these cells, has been previously reported (Jones, et al., 1973).

ULTRASTRUCTURAL EXAMINATION

In 10 day control mice many granule cells were in their definitive location (Figs. 3A, 4A, 4B, 5A). Within the molecular layer, myriads of parallel fibers were present along with Purkinje cell dendrites and Bergmann astroglial processes (Fig. 10). Numerous mature parallel fiber-Purkinje cell contacts surrounded by a Bergmann astroglial matrix were observed (Fig. 11). In all mice (saline or MAM-injected) parallel fiber presynaptic terminals (varicosities) were observed containing round synaptic vesicles making normal synaptic contact with Purkinje cell dendritic spines that demonstrated a postsynaptic thickening with a synaptic cleft of 200 - 300 Å.

In some areas of the molecular layer the parallel fibers were absent; leaving Purkinje cell dendrites with naked spine specializations surrounded by a glial matrix (Fig. 12) (similar to those described by Hirano and Jones (1972) in 25 day cycasin). Naked Purkinje cell dendritic spines with postsynaptic thickenings were occasionally observed in all 10 day saline-injected mice (This phenomenon has not been previously reported.) (Fig. 13).

Growth cones were exhibited in all saline-injected 10 day mice (Fig. 14) (similar to those observed in the rat at varying ages, del Cerro and Snider, 1968). However, these were seen in only one of the five MAM-treated 10 day mice.

In contrast to previous observations in this laboratory (Jones, et al., 1973), necrotic cellular elements persisted within the external differentiating cell layer and molecular layer (Fig. 15). These appeared to be engulfed by astrocytes or differentiating cells. Membranous whorls composed of smooth concentric membranes were occasionally observed within astrocytes in both groups (saline or MAM-injected) of mice (Fig. 16). However, no evidence of degeneration of presynaptic terminals was seen in either group (saline or MAM-injected) of mice.

Figure 3. Two sagittal sections from 10 day control (3A) and MAM-injected mice (3B) show the differences between the cerebellar vermis morphology. Note the reduction in size of the vermis, lack of an external differentiating and granule cell and Purkinje cell layers as well as the simplicity of folia in the MAM-injected mouse cerebellar vermis. The loss of cells following MAM-injection is not always this complete. By 10 days of age, a layer of regenerating cells is often seen in many folia. Cell regeneration was extensive in the present experiment. These tissue sections are from a previous pilot experiment with an identical design for injections at day zero and for perfusion at day 10. Paraffin embedded, 10 um sectioned, H&E stained, 33 x.

3A

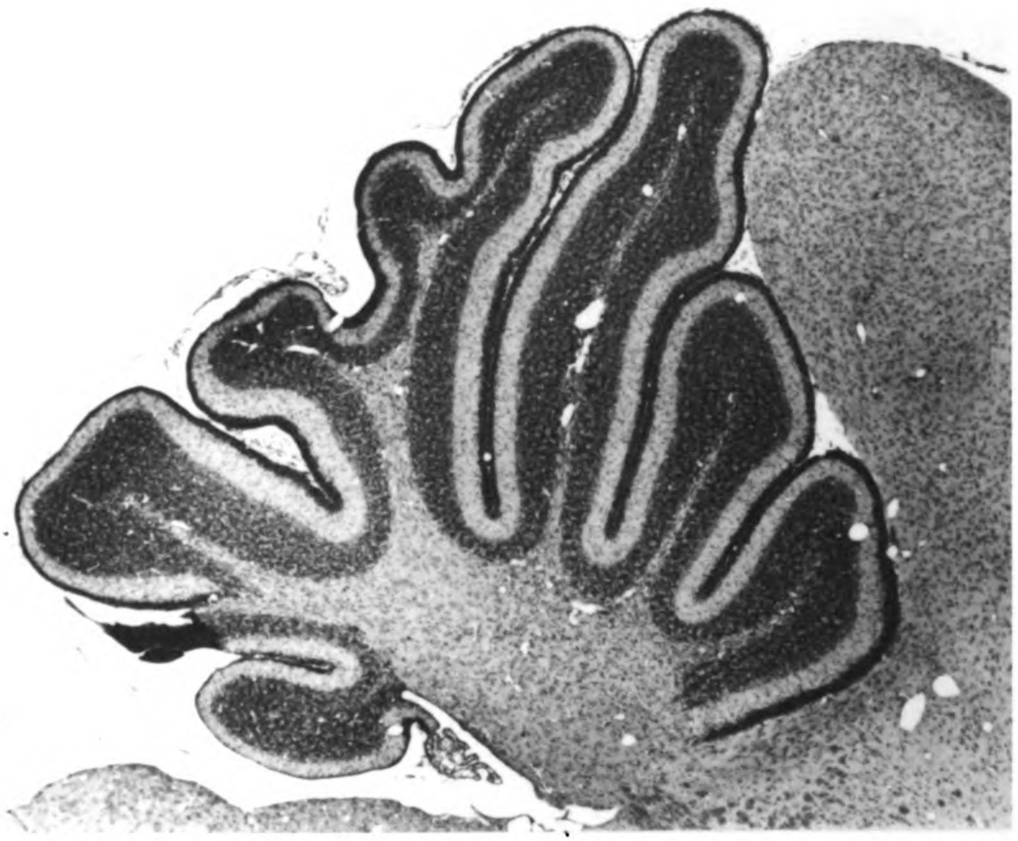

B

500um

Figure 4. Comparison of cerebellar folia in 10 day saline and MAM-injected mice shows architectural differences resulting from loss of differentiating cells in the treated animals. When compared to controls (4A and B), the external differentiating cell layer (DL) is almost nonexistant in some areas. Concomitant dislocation of the Purkinje cells (arrows) results in an apparent absence of the molecular cell layer in many areas of the MAM-injected mice (4C and D). Note the paucity of cells in the internal granule cell layer region of treated mice. Regeneration of external differentiating cells has partially repopulated areas of the sulci within figure 4C. Molecular layer, ML; Purkinje cell layer, PL; internal granule cell layer, IGL. 4A, paraffin embedded, 10 um sectioned, H&E stained, 170 x. 4B, 4C, 4D, Epon-araldite embedded, 1 um sectioned, toluidine blue stained, 170 x.

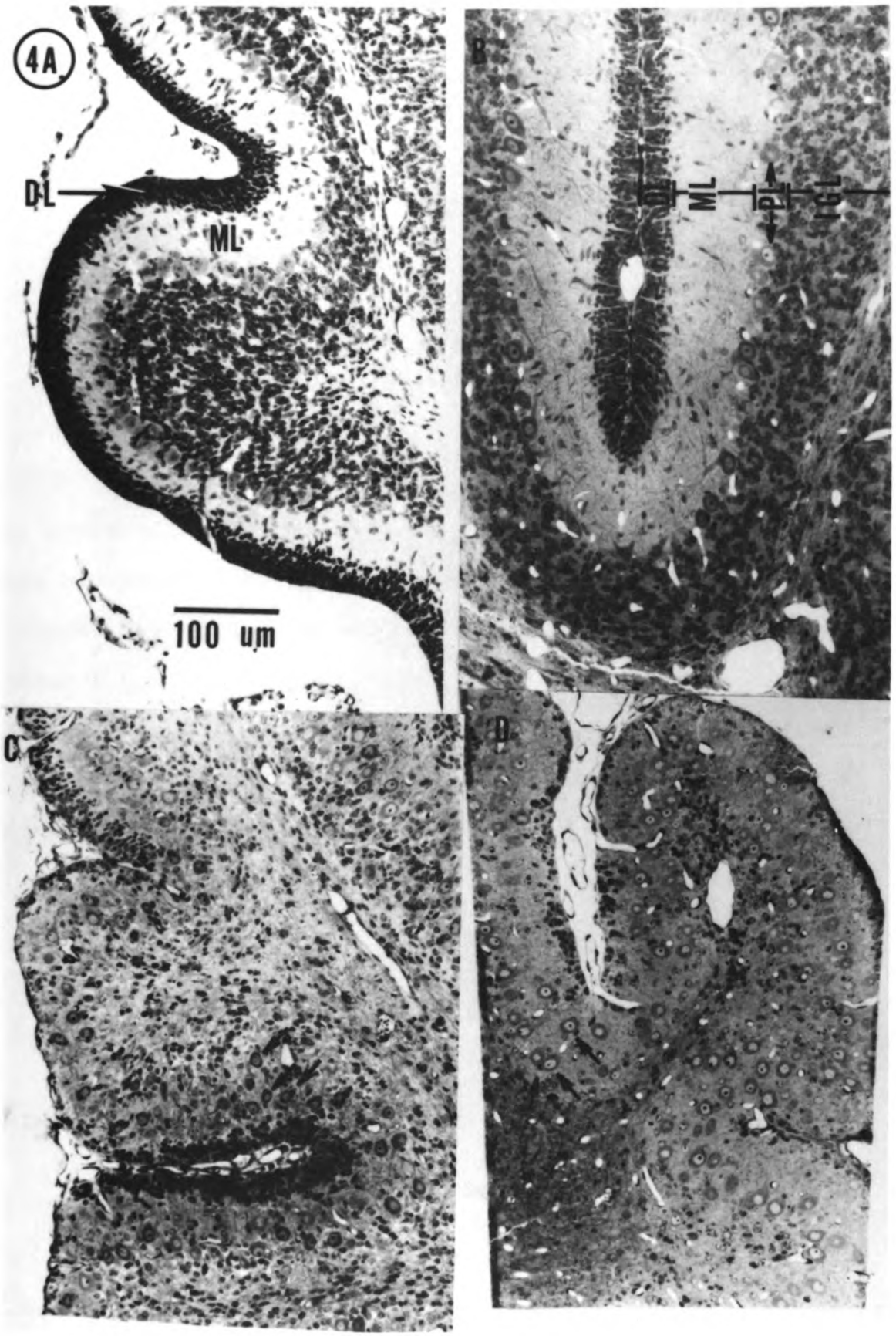
4A
DL
ML
100 um
B
ML
PL
IGL
C
D

Figure 5. The random array of Purkinje cell somata (PC) in the molecular and reduced internal granule cell layers in 10 day MAM-injected mouse cerebellums (5B) contrasted sharply with the orderly arrangement of the external differentiating cell (EL), molecular (ML), Purkinje cell (PL) and internal granular cell layers (IGL) in the control (5A). Also notice the absence of a portion of the external differentiating cell layer (EL) in the MAM-injected mouse. Epon-araldite embedded, 1 um sectioned, toluidine blue stained, 320 x.

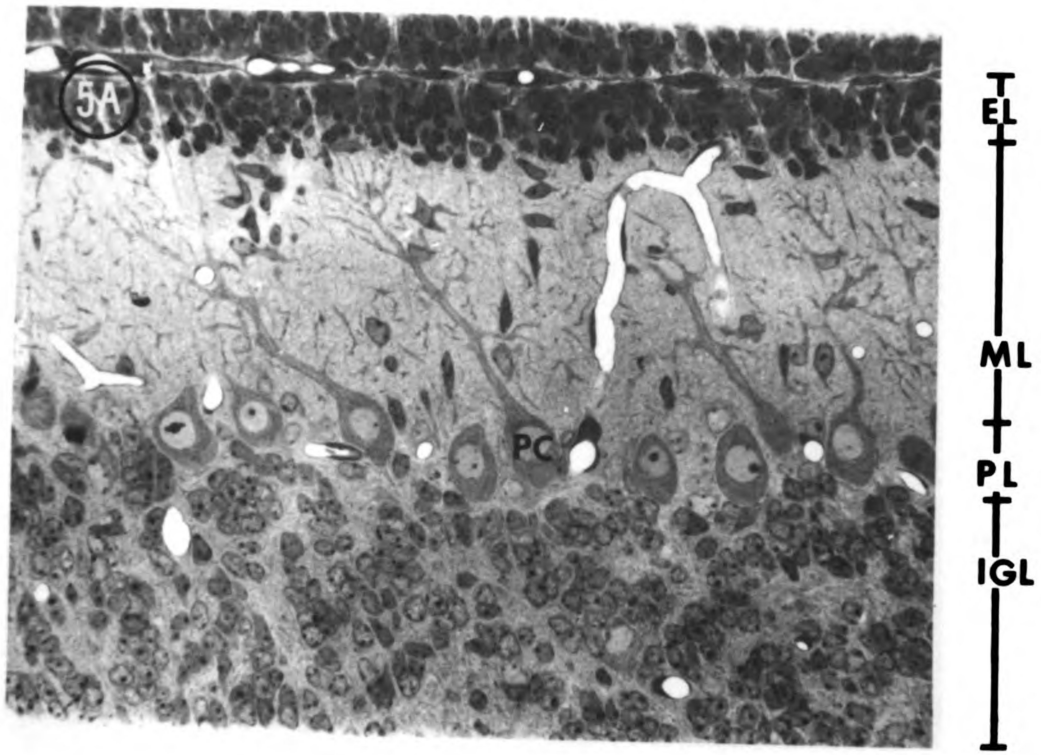

100 um

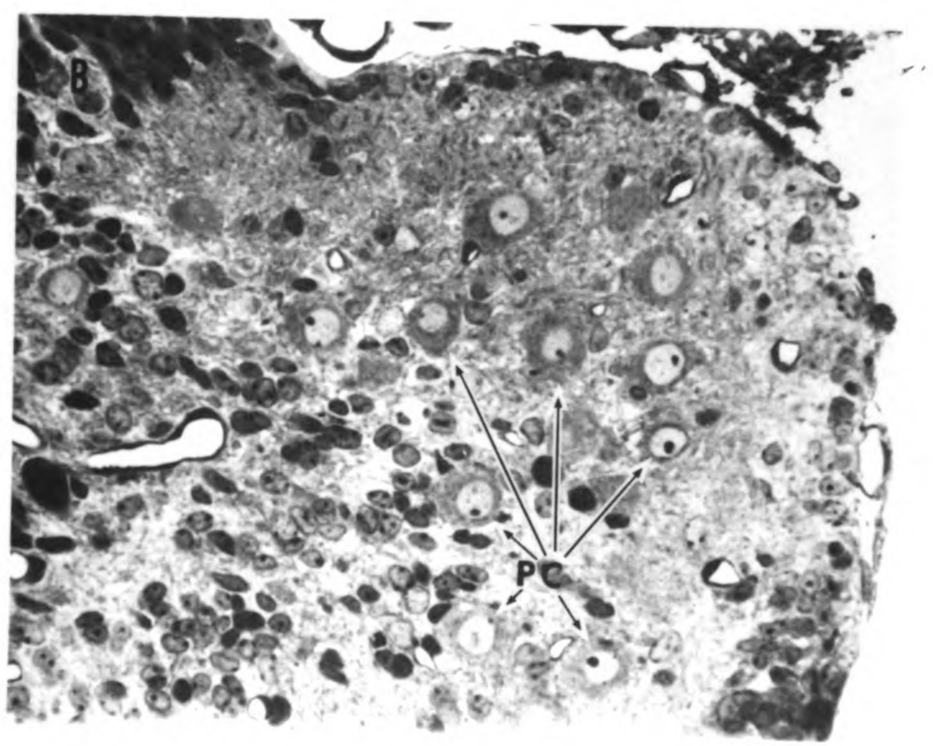

Figure 6. Disorientation of Purkinje cell apical poles is consistently observed in MAM-injected 10 day mice. These photomicrographs (6A and B) illustrate the random orientation of the apical poles of Purkinje cell dendrites (arrows) in two MAM-injected mice, (6A) in the crest of a folium and (6B) in the depth of a sulcus. The variability in the differentiating cell (DL) loss and regeneration is illustrated as well as the Purkinje cell architectural disarray. Epon-araldite embedded, 1 um sectioned, toluidine blue stained, 400 x.

6 A

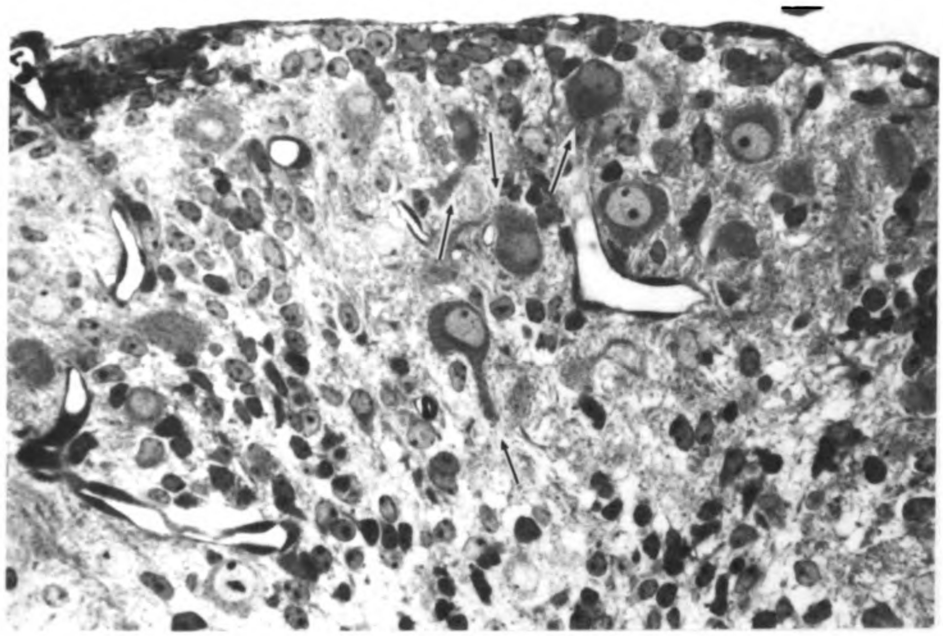

100 um

B

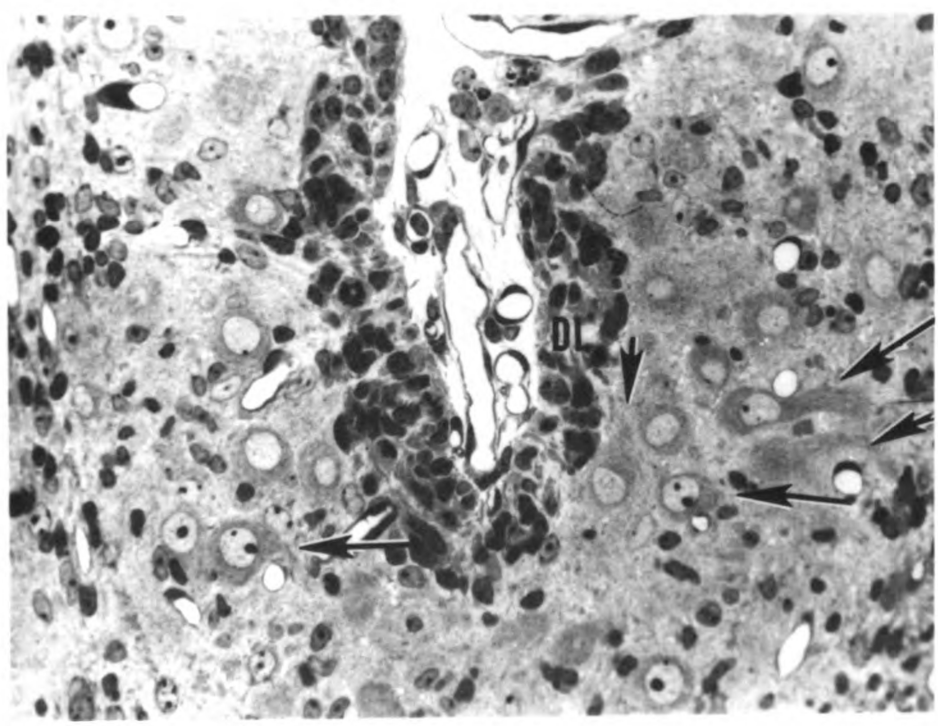

Figure 7. Comparison of Purkinje cells and dendrites in 10 day saline and MAM-injected mice (Rapid Golgi technique). 7A is a montage of a Golgi impregnated Purkinje cell soma and its single dendritic tree from a saline-injected mouse cerebellum. A through focus examination of this tissue section revealed a single dendritic tree with a main primary dendrite and remnants of one or possibly two other primary dendrites passing from the Purkinje cell soma. Three Purkinje cell somata are present (PC); one is impregnated and two others are not (small arrows). Spines are observed on branches of the dendrites (box). 7B is a Purkinje cell soma with four massive Primary dendrites (arrows) exhibiting fewer secondary and tertiary branches and branchlets with spines (box) in the MAM-injected mouse. Notice its axon (AX). PC, Purkinje cell soma, Rapid Golgi impregnation technique, 920 x.

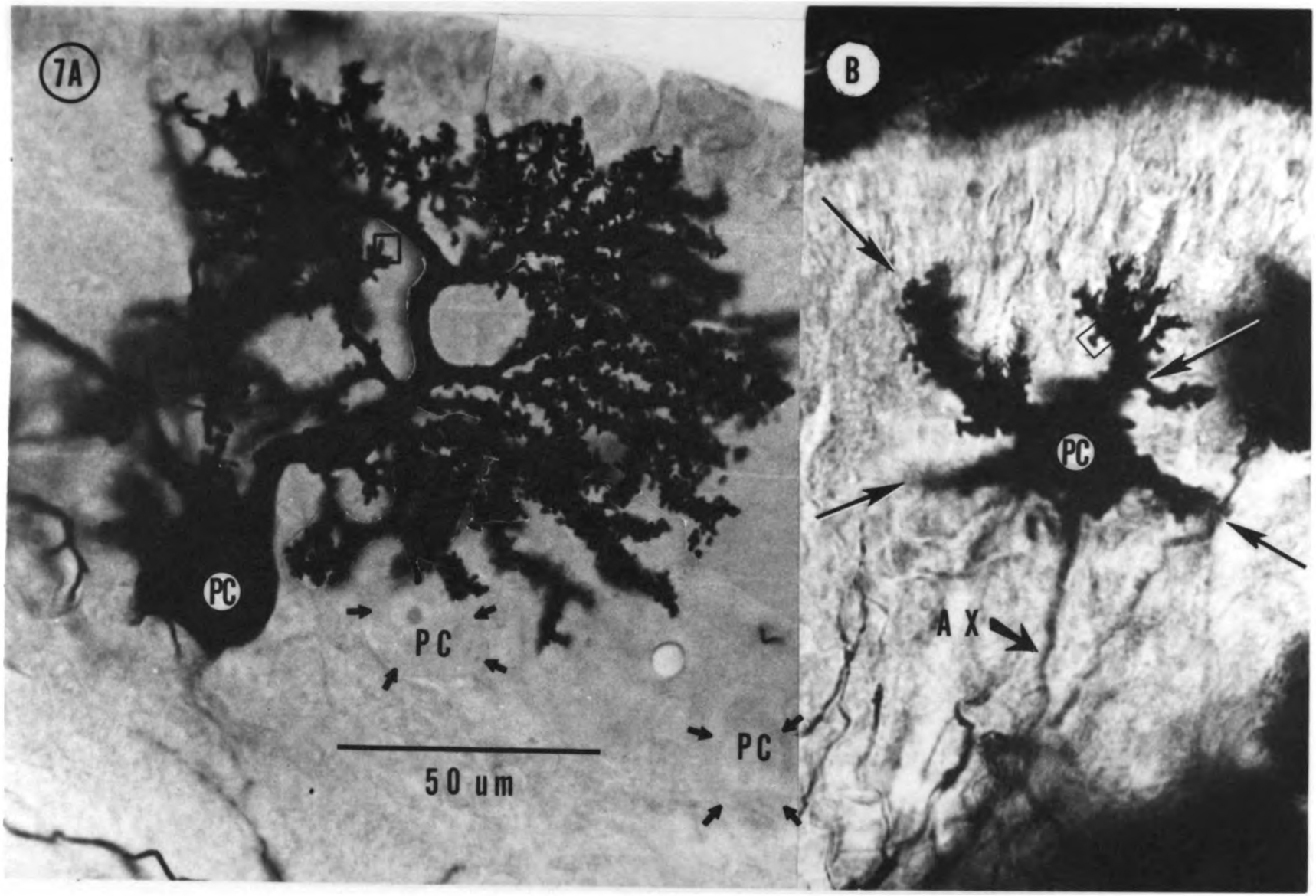
7A
PC
PC
PC
50 um
B
PC
AX

Figure 8. The disorientation of two Purkinje cell somata and their dendrites in 10 day MAM-injected mice is illustrated in 8A and B. Notice the variability in the distance of Purkinje cell somata (PC) from the meninges, (Me) and the Purkinje cell dendritic distribution in three dimensions. Compare this to the normal Purkinje cell dendrites that are planar with their soma around 100 um from the pial-glial surface (Fig. 7A). 8A illustrates a Purkinje cell soma (PC) with dendrites (arrows) growing in abnormal directions towards the internal granule cell layer. 8B illustrates another Purkinje cell soma (PC) about 75 um from the pial-glial membrane (Me) with four primary dendrites (arrows) growing in different directions and planes. Rapid Golgi impregnation technique, 75 um sectioned, 920 x.

Figure 8. DISORIENTATION OF PURKINJE CELL DENDRITES IN MAM INJECTED 10 DAY MOUSE CEREBELLUM.

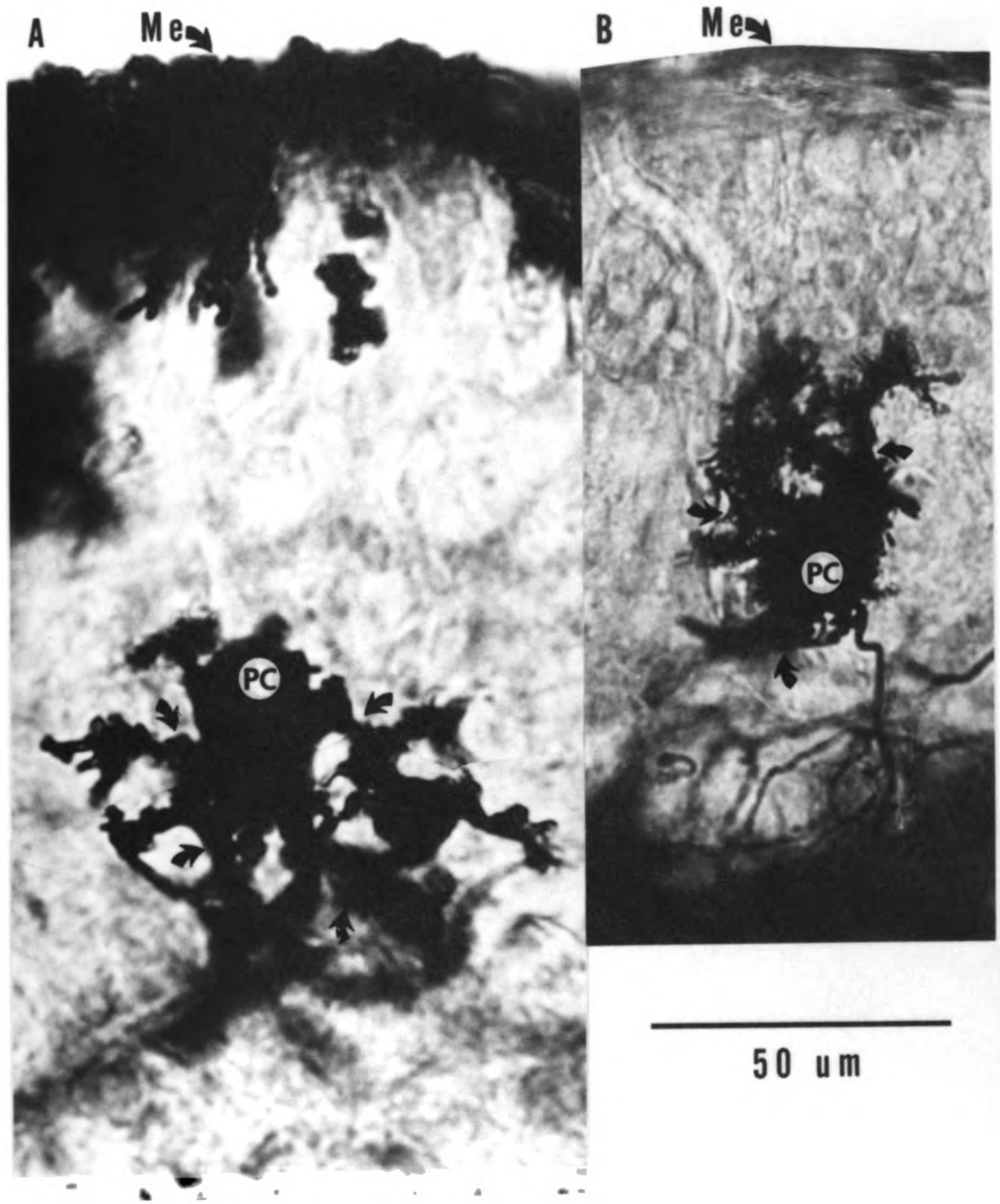

Figure 9. Golgi epithelial (Bergmann) cells.
Normal Golgi epithelial cells (GEC) give off lateral processes with warty excrescences (arrows) on the vertically directed processes as they pass towards the pial-glial membrane (A1, A2). In MAM-injected mice the lateral processes are either greatly reduced in number or virtually absent. The lengths of the vertical processes in cerebellums of MAM-injected mice appear to be reduced when compared to the normal (B1, B2, C). Rapid Golgi impregnation technique, 75 um sectioned, 680 x.

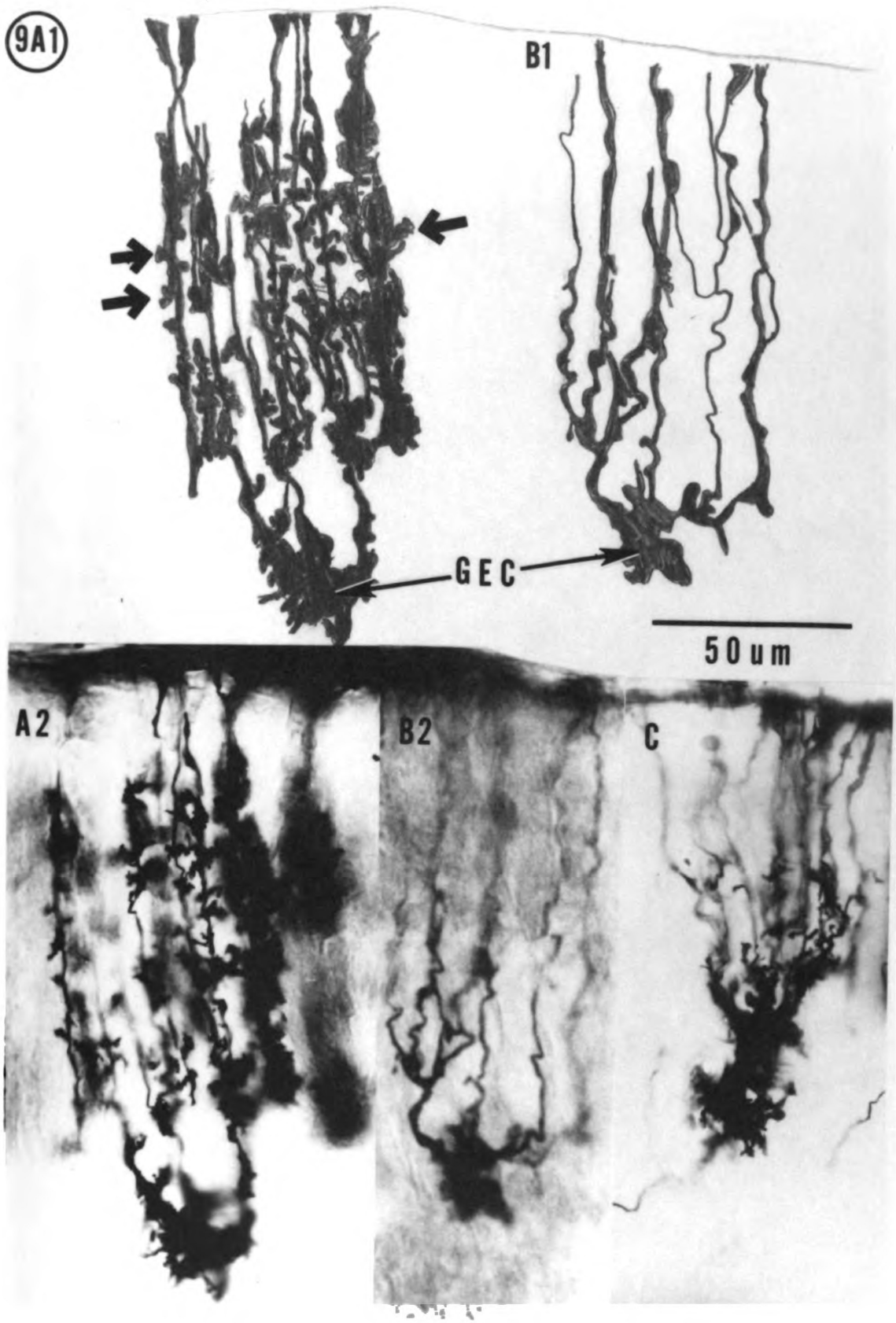
9A1
B1
GEC
50um
A2
B2
C

Figure 10. External differentiating layer and molecular layer in control 10 day mice. This electron micrograph of the superficial region of the molecular layer and the external differentiating cell layer illustrates the myriads of parallel fibers (pf) cut in cross section, Bergmann astroglial processes (GL), small portions of a Purkinje cell dendrite (Pc d) and the meninges (Me). At the meninges, a neuroglial end-foot is present (GLF) forming the sub-pial portion of the glial limiting membrane. Cells within the external differentiating cell layer assume a variety of shapes as they mature into neuroblasts and undergo mitotic division prior to migration towards their definitive location within the internal granule cell layer. Uranyl acetate en-bloc stained, Epon-araldite embedded, grids stained with uranyl acetate and lead citrate, 7200 x.

(10)

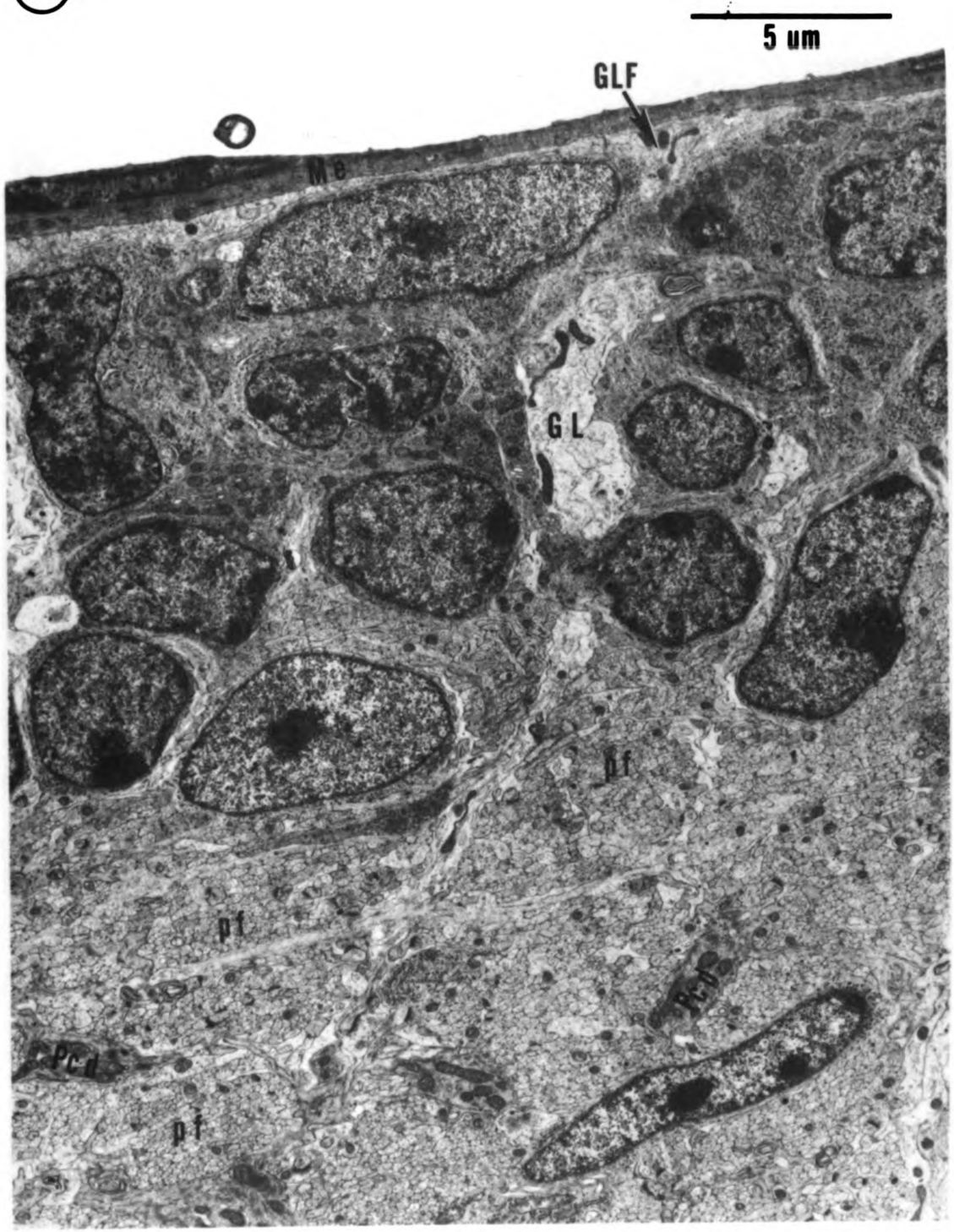

Figure 11. Molecular layer in 10 day control mice. This is a higher magnification of a section from figure 10 illustrating the relatively electron dense Purkinje cell dendrite (Pc d) surrounded in part by Bergmann astroglia (GL) and parallel fibers (pf). Notice the numerous parallel fiber-Purkinje cell dendritic spine synapses (PS) each surrounded in part by a Bergmann astroglial matrix. Uranyl acetate en-bloc stained, Epon-araldite embedded, grids stained with uranyl acetate and lead citrate, 11,700 x.

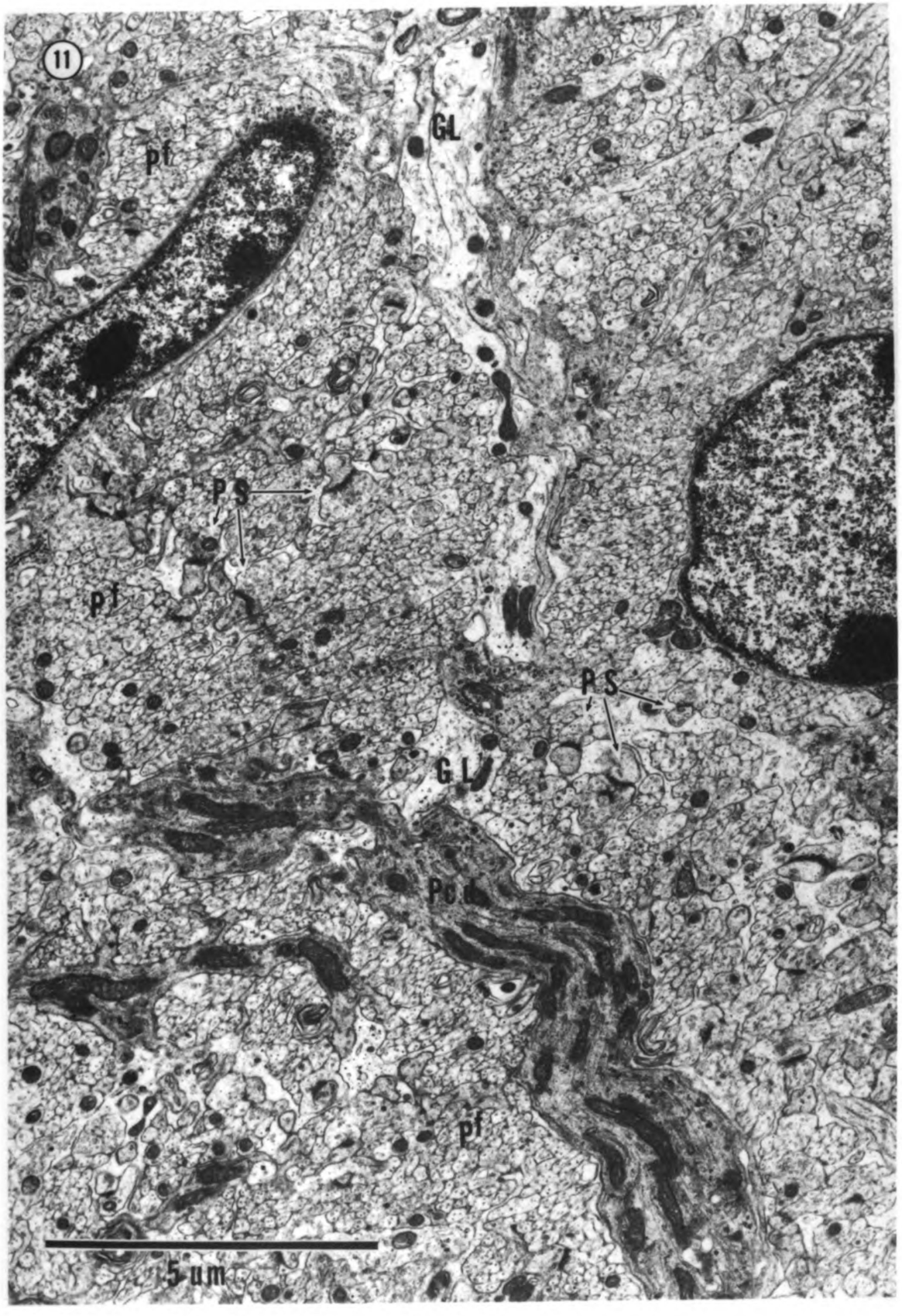
11
GL
pf
PS
pf
PS
GL
Pc
pf
5 um

Figure 12. Naked Purkinje cell dendritic spines in 10 day MAM-injected mice. Purkinje cell dendrites (Pc d) with naked spines (NS) surrounded by a glial matrix (GL) are seen in areas of the molecular layer where the parallel fibers are absent (12A and B). Naked spines (NS) on Purkinje cell dendrites have postsynaptic thickenings (arrows) contacted by Bergmann astroglial matrix (GL) rather than parallel fiber presynaptic varicosities. Uranyl acetate en-bloc stained, Epon-araldite embedded, grids stained with uranyl acetate and lead citrate, A. 26,000 x, B. 30,000 x.

Figure 13. Naked spines from 10 day control mice. Naked Purkinje cell dendritic spines with postsynaptic thickenings surrounded by Bergmann glial matrix were occasionally observed in all 10 day control Swiss albino mice. 13A and B show naked spines (NS) with postsynaptic thickenings (arrows) surrounded by a glial matrix (GL) with parallel fibers (pf) in the vicinity. No differences from naked spines seen in MAM-injected mice are apparent. Uranyl acetate en-bloc stained, Epon-araldite embedded, grids stained with uranyl acetate and lead citrate, A. 54,000 x, B. 27,000 x.

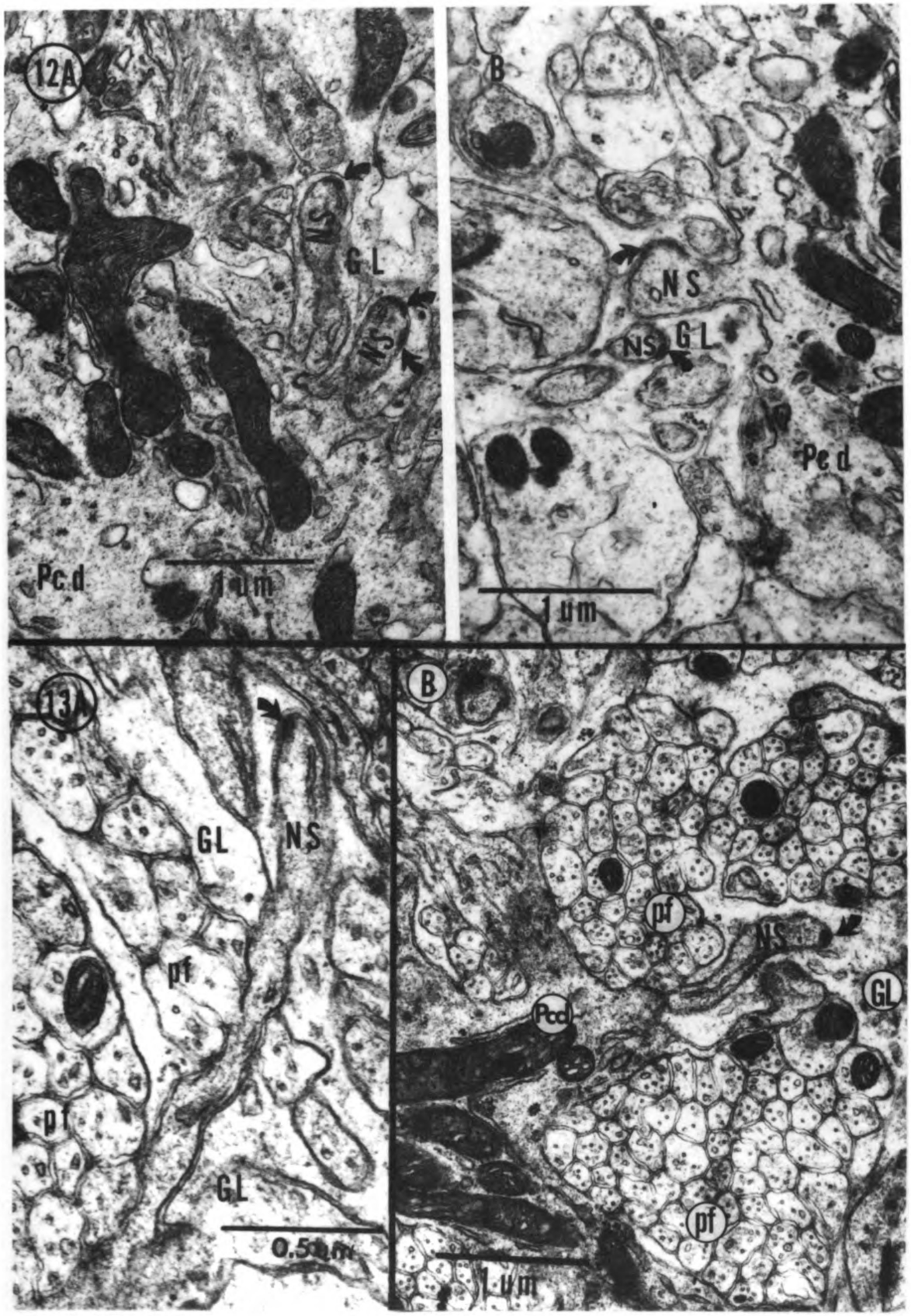
12A
NS
GL
NS
Pc d
1 um
B
NS
NS
GL
Pe d
1 um
13A
GL
NS
pf
pf
GL
0.5 um
B
pf
NS
GL
Pcd
pf
1 um

Figure 14. Growth cones in 10 day Swiss albino mice. This illustrates a Purkinje cell dendrite (Pc d) and two growth cones (GC) containing vacuoles 500 - 1100 Å in diameter, surrounded by a Bergmann glial matrix in a 10 day saline-injected mouse. Synaptic vesicles (sv) 240 - 440 Å in diameter within a mature synaptic terminal can be compared with the vacuoles within the growth cones. Uranyl acetate en-bloc stained, Epon-araldite embedded, grids stained with uranyl acetate and lead citrate, 26,000 x.

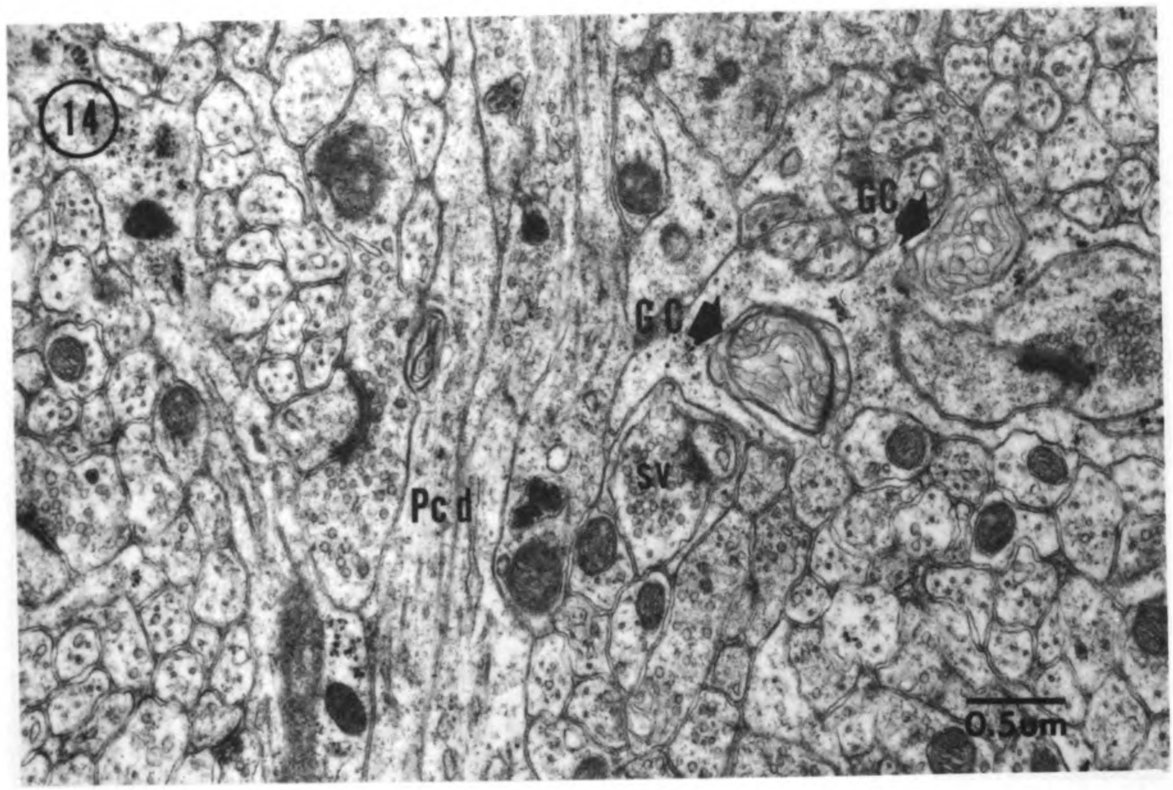
14
GC
GC
Pc d
sv
0.5um

Figure 15. Residual MAM-induced cellular destruction in 10 day mice. Necrotic debris, remnants of the cellular destruction due to the zero day injection of MAM still persists. 15A is a low power electron micrograph illustrating the persistent or regenerating external differentiating cells as well as degenerating cells (Dd) apparently engulfed by a differentiating cell, and a dense body (Db) next to a normal nucleus. 15B illustrates debris engulfed by the watery cytoplasm of an astrocyte (As) surrounded by a number of normal external differentiating cells. 15C illustrates a cell with the appearance of an astrocyte (note nucleus, N) containing dense bodies (Db) and cell debris of many dead cells surrounded by a pale cytoplasm. Uranyl acetate en-bloc stained, Epon-araldite embedded, grids stained with uranyl acetate and lead citrate, A. 2,700 x, B. 5,400 x.

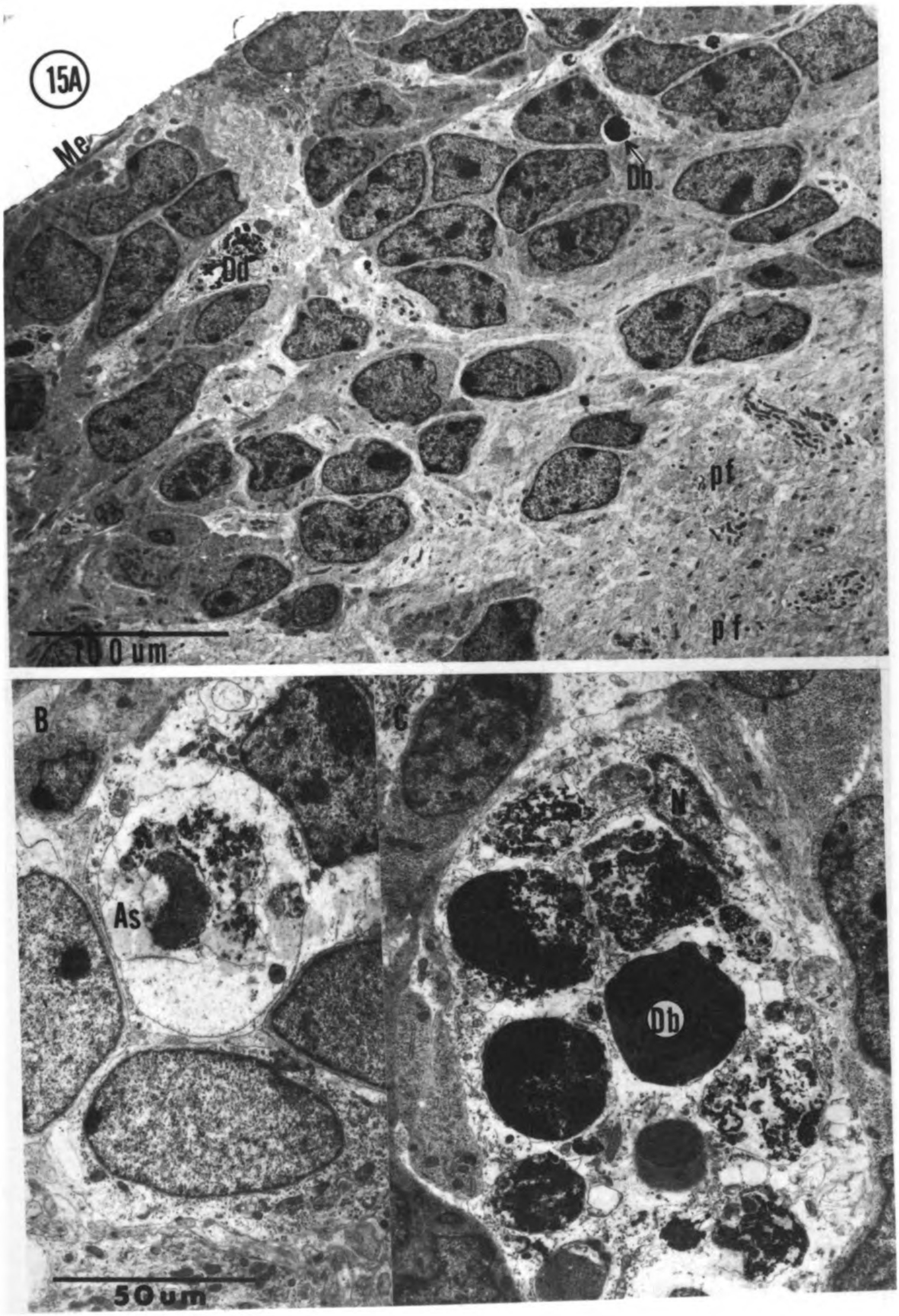
15A
Me
Db
Dd
pf
pf
100 um
B
As
50 um
C
N
Db

Figure 16. Membranous whorls in 10 day saline-injected Swiss albino mice. 16A illustrates a membranous type of whorl (MW) derived from the endoplasmic reticulum occasionally observed within Bergmann astrocytes near the pial-glial membrane. In contrast, 16B illustrates a postsynaptic spine containing an artifactual type of whorl that surrounds other vacuoles (V). Whorls are occasionally observed surrounding other structures such as mitochondria. They may also exhibit an empty cytoplasm within the whorl. Uranyl acetate en-bloc stained, Epon-araldite embedded, grids stained with uranyl acetate and lead citrate, A. 39,000 x, B. 36,000 x.

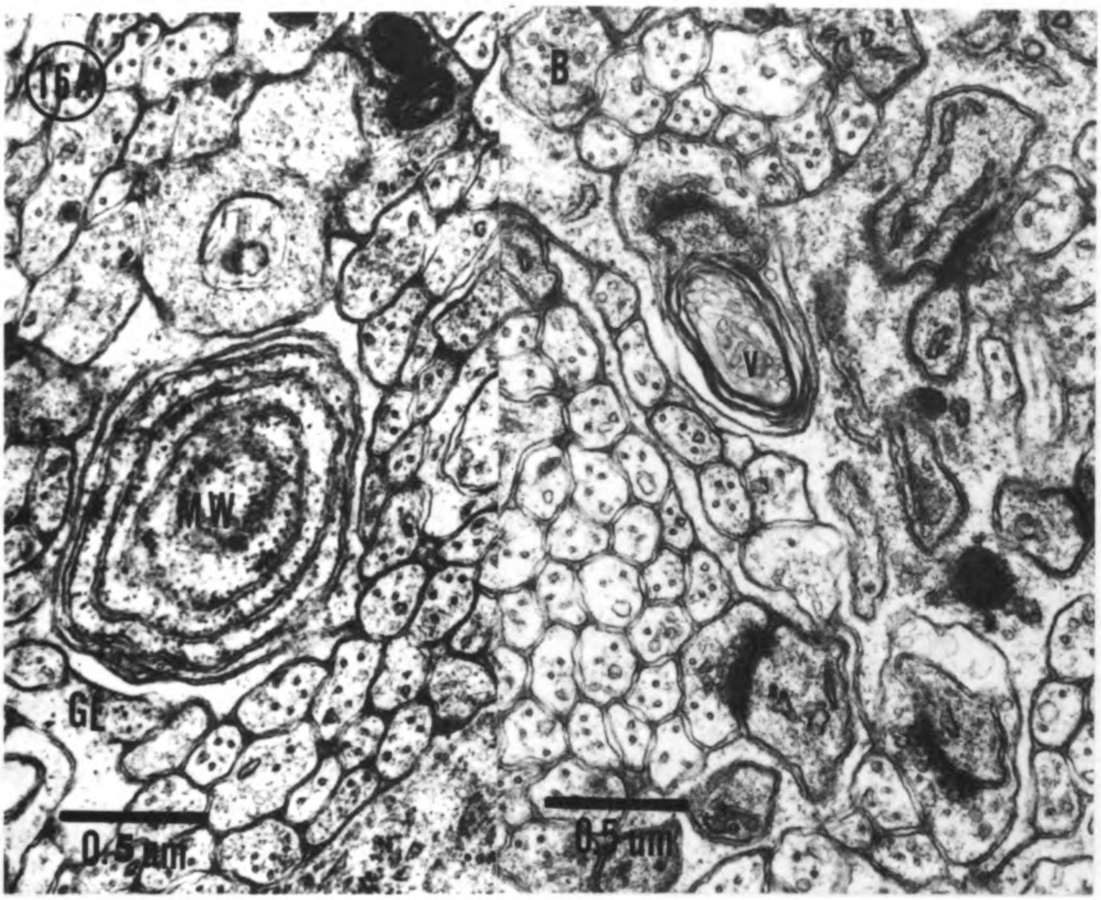
T6A
B
V
MW
GL
0,5 µm
0,5 µm

DISCUSSION

PHYSICAL EXAMINATION

The mice injected at day zero weighed approximately 1.7 grams. At 10 days, the general activity of the MAM-injected and saline-injected mice was equal, while the average weight of the saline-injected animals was 6.19 $\pm$ 0.58 grams, and the MAM-injected animals weighed 5.22 $\pm$ 0.84 grams. At day 10 all of the saline-injected mice had smooth white hair, while only one of the six mice in the MAM-injected group exhibited any hair. Both groups exhibited equal tremor of the head and neck, and also demonstrated equal climbing and righting abilities. At day 10, three out of eight saline and none of the MAM-injected mice positioned their legs normally with legs tucked underneath.

As normal mice mature, they gain weight, slowly lose their tremor, grow hair, open their eyes, and position their feet underneath themselves. The decreased weight gain among the 10 day MAM-injected mice when compared to the controls reflected the general effects of MAM on total body growth. This effect has been corroborated by Jones, et al. (1972a). The remaining physical changes seen in the 10 day mice were also consistent with those observed in an early pilot experiment by Jones, et al. (1972a), that determined the effects of cycasin (0.5 mg/gm body weight) on mice. They observed a delay by a few days in the appearance

of the fur and/or the opening of the eyes in the treated mice, even though the climbing and/or righting abilities were not impaired.

The weight gain, tremor, growth of hair, opening of the eyes, and the proper positioning of the feet reveal the gradations of maturity in the Swiss albino mice. Therefore, in this experiment at 10 days, the MAM-injected mice appeared more immature than their saline-injected littermates. Histological changes within the cerebellum of MAM-injected mice reflect a more specific action on the dividing cells in this location and can not be attributed to the general effects of the agent on growth and development.

MACROSCOPIC EXAMINATION

Sagittal sections of the vermis in eight MAM-treated and five control mice at 10 days of age when measured revealed a 60% reduction in the sagittal area of the vermis in the MAM-injected mice (Fig. 2). Woodward, et al. (1975) measured the sagittal sections of the vermis in rats at varying postnatal ages after injecting rats with MAM (10 mg/Kg body weight) for four consecutive postnatal days. At postnatal day four the sagittal sections were only 12% less than control. This is a period when only a few granule cells have undergone differentiation and eventual destruction. At day 7, there was a 35% decrease in the MAM-injected rat sagittal areas of the vermis. This was presumed to be

due to the diminished external differentiating cell layer. At postnatal day 14, the reduction was diminished to 29%.

Comparison of the amounts of MAM used by Woodward, et al. (1975) with those in this investigation, reveals that the variability of the reductions in the vermis may be due to the dosage and sequence of MAM injections. It has been shown that one massive dose of MAM (50 mg/Kg or 0.05 ul/gm body weight) produces a greater reduction in the sagittal area of the vermis in the mice at 10 days than four consecutive smaller doses (10 mg/kg body weight) in the rat taking into account the species difference.

LIGHT MICROSCOPIC EXAMINATION OF THE CEREBELLAR CORTEX

Not only was there a reduction in the cross sectional area of the vermis at 10 days in the MAM-injected mice, but the normal histological architecture was altered. In many areas of the vermis in the 10 day MAM-injected mice, the external differentiating cell layer or the internal granule cell layer could not be identified (Fig. 3). The putative molecular layer was occupied by dislocated Purkinje cells that appeared to be of the same diameter as those in the control mice.

Purkinje cells

1. Dislocation of Purkinje cell somata

A striking feature of 10 day MAM-injected mice was the dislocation of Purkinje cell somata within the molecular and

internal granule cell layers. The Purkinje cell somata disorientation has been the subject of many publications but the explanation remains unclear. One theory for the disorientation describes the elimination of external differentiating and internal granule cells (Altman and Anderson, 1973; Herndon, et al., 1971; Rakic and Sidman, 1973a; Woodward, et al., 1975). These processes interrupt the development of the external differentiating cell layer and the folial expansion that would provide sufficient area for a normal Purkinje cell layer to develop. Woodward, et al. (1975) reported that even though a certain amount of regeneration takes place within the external differentiating and internal granule cell layer, the regeneration may occur after the Purkinje cells have lost their migratory capabilities, leaving their somata in a definitive aberrant location.

Norman (1940) hypothesized that Purkinje cell disorientation observed in cases of congenital cerebellar hypoplasia is correlated with the absence of granule cells or their abnormal migration. He implicated the role of astrocytes in the misalignment. Recently, Jones and Gardner (1976) reported a second theory for Purkinje cell somata disorientation. They stated that the rapidity with which the misalignment occurs suggests that the glial reaction has a more definitive role than abnormal migration or reduction of granule cells. They attribute this glial reaction to "astrocyte swelling" which is "the only obvious

event which induced the disorientation pattern of Purkinje cells."

Both theories appear logical. I believe that the misalignment is due to a combination of these events rather than exclusively one or the other. Therefore, the folial immaturity due to the external differentiating cell layer destruction, coupled with the "astrocytic swelling" that places further space limitations within the molecular layer, result in the random arrangement of Purkinje cell somata.

2. Random Purkinje apical poles orientation

Purkinje cell apical poles (the initial portions of primary dendrites) were randomly oriented in MAM-injected mice (Fig. 6). Altman and Anderson (1972) hypothesized that with destruction of the external differentiating cell layer the apical poles of the Purkinje cell somata, which normally point towards the surface, become randomly oriented. "The observation indicates that, whereas the growth of the apical cone (pole) of Purkinje cells is an autonomous event, the normal orientation of this growing structure depends on the presence and location of the external germinal layer" which acts as an "attractive force" (Altman and Anderson, 1972). The presence of an "attractive force" has not been biochemically substantiated to date, but I believe that this theory is a plausible

explanation for the random orientation of Purkinje cells in 10 day MAM-injected mice.

3. Many massive primary dendrites

In MAM-treated mice, many massive primary dendrites projected from each Purkinje cell and appeared larger in diameter than the one or two primary dendrites observed in the saline-injected mice (Figs. 7 and 8). This finding is consistent with the previously reported work of Woodward, et al. (1975) which goes one step farther by suggesting a hypothesis for the formation of multiple primary dendrites. In the absence of parallel fibers in an agranular cerebellum, dendritic growth may be spread from several early Purkinje somatic projections. With the late appearance of large numbers of parallel fibers in treated animals, one or more Purkinje cell processes may develop into a dendrite with secondary and tertiary branches. They continue by stating that if the target of a particular dendrite is not reached, multiple primary dendrites continue to grow larger and become progressively more difficult to absorb. The same authors proposed that in the absence of a favorable environment, the immature growing processes of the dendrites (filopodia) will grow farther distances from the soma than normal, to a more suitable environment, before they begin their maturation into secondary and tertiary branches and branchlets with spines.

4. The Purkinje cell dendrite

In the present study, 10 day MAM-injected mice exhibiting many massive primary dendrites also had fewer than normal secondary and tertiary dendritic branches and branchlets. They were distributed in three dimensions, which contrasted to the fewer planar dendrites observed in 10 day control mice. The dendritic branches assumed a variety of shapes in MAM-injected mice. The shapes appeared to depend upon the positions of the cell bodies within the cerebellar cortex (superficial or deep) and on the orientation of the apical pole (Fig. 6). This is in agreement with numerous reports (Altman and Anderson, 1971, 1972; Mouren-Mathieu and Colonnier, 1969; Woodward, et al., 1975).

The random orientation of the Purkinje cell somata as well as their primary dendrites and the autonomous growth of the dendrites account for the unusual shapes of the arborizing dendrites (Altman and Anderson, 1972; Woodward, et al. 1975). The "weeping willow" type of Purkinje cell dendrite is due to the downward differentiation of dendrites that have arisen to the pial-glial surface from a Purkinje cell soma located nearer to the surface than normal (Shofer, et al., 1964; Hamori, 1969). An apical pole that is oriented sideways may cause the primary dendrite to course parallel to the pial-glial surface while another apical pole oriented towards the medullary region of the cerebellum may result in the inward orientation of a dendrite after maturity (Altman

and Anderson, 1972; Woodward, et al., 1975). Thus, I agree with Altman and Anderson (1972) that the three-dimensional random orientation of the developing dendrites is due to the absence of the "attractive force" of the external differentiating cell layer which has led to the random orientation of the apical pole and primary dendrite.

Compared to 10 day control mice, a reduction in the length of the Purkinje cell dendrites was observed in silver impregnated vermis sections obtained from the MAM-treated mice. With the reduction in the number of secondary and tertiary branches and branchlets, along with this reduction in length, there was a concomitant decrease in the number of spines photomicroscopically present (Figs. 7 and 8). During the first seven postnatal days, the dendrites normally grow in length, become oriented in a characteristic way, and divide into secondary and tertiary branches. During postnatal days 8 - 11, the Purkinje cell dendrites continue to grow and may contain one or more primary dendrites (Dvorak and Bucek, 1970). Purkinje cells mature towards the end of the second postnatal week with the formation of dendritic spines clearly visible at 10 days postnatally (Meller and Glees, 1969). As a result of MAM-administration, the growth and development of the Purkinje cells in 10 day MAM-injected mice corresponds to the maturity observed in six to eight day control mice (Meller and Glees, 1969). Therefore, the reduction rather than the overgrowth in length of

the Purkinje cell dendrites as well as the reduced number of dendritic spines in the 10 day MAM-treated mice appears to reflect the abnormal maturation within the cerebellar cortex.

External differentiating cell reduction and regeneration in MAM-treated mice

Research within the past years has shown that the external differentiated granule cells of the postnatal cerebellum are susceptible to the action of MAM (Chanda, et al., 1975; Hirano, et al., 1972; Hirano and Jones, 1972; Jones, et al., 1972a, 1973). In this research, we observed the almost total absence of external differentiating cell layer in many cerebellar folia of 10 day MAM-injected mice, which was earlier described (Jones, et al., 1972a, 1973). Many cerebellar lobules within MAM-injected mice appeared to contain fewer than normal internal granule cells (Figs. 3, 4,5,6). Those internal granule cells that were present in MAM-injected mice appeared to be the same size (7 - 10 um) in diameter when compared with 10 day control mice. Thus, we concur with others who have shown that upon MAM administration into zero day animals, the external differentiating cells are destroyed causing the subsequent reduction in internal granule cells and their processes (Chanda, et al., 1975; Hirano, et al., 1972; Hirano and Jones, 1972; Jones, et al., 1973; Matsumoto, Spatz and Laqueur, 1972; Shimada and Langman, 1970).

Other folia in 10 day MAM-injected mice contain an almost normal appearing external differentiating cell layer, which contrasts with the observed reductions in the adjoining internal granule cell layer and the random orientation of Purkinje cell somata. Shimada and Langman (1970) hypothesized that the cells that escape MAM destruction and regenerate to repopulate areas of the external differentiating cell layer, are not in an active "DNA synthetic phase". The DNA synthetic phase in the mouse lasts six to eight hours in contrast to a complete cell cycle of 20 hours (Shimada, 1966). Since MAM is active only a few hours, a single dose will normally only destroy 25 - 40% of those cells within the external differentiating cell layer by this mechanism (Shimada and Langman, 1970). The remaining cells may regenerate. The almost normal appearing areas of the external differentiating cell layer within 10 day MAM-injected mice therefore may be due to the prolific regeneration of those external differentiating cells that escaped the effect of the MAM-treatment.

Golgi epithelial (Bergmann) astroglia

With the reduction and subsequent regeneration of external differentiating and internal granule cells in MAM-injected mice, some changes are observed within the Golgi epithelial (Bergmann) cells and their processes. Ten day MAM-injected mice Golgi epithelial (Bergmann) cells were observed within the outer portion of the inner granule

cell layer giving off vertical processes that passed in an occasional oblique course towards the pial-glial membrane. When comparing MAM mice with the saline-injected 10 day control mice, the lengths of the vertical processes appeared to be reduced in length. The lateral processes with warty excrescences, normally upon the Bergmann fibers, were greatly reduced or virtually absent in 10 day MAM-injected mice. Sotelo and Changeux (1974) observed smooth contoured ascending fibers in the bottom two-thirds of the molecular layer. The fibers in the upper one-third of the molecular layer exhibited the typical cytoplasmic excrescences in 22 day old homozygous Weaver mice. "The Bergmann fibers often do not show the straight and perpendicular orientation characteristic of these fibers, but have an oblique course". Their observations of Bergmann fibers were similar to those examined in this study of 10 day MAM-injected mice.

Necrotic debris in 10 day MAM-injected mice

Engulfment of necrotic debris by Bergmann fibers was demonstrated within the external differentiating cell layer and has been previously reported by several investigators in both normal and experimentally induced cell necrosis (Herndon, 1968; Jones and Gardner, 1976; Shimada and Langman, 1970). Necrotic debris surrounded by a pale watery cytoplasm of an astrocyte has also been observed within the normal differentiating hippocampus (Jones and Brownson, 1969). Acute injury to the differentiating cerebellum and

cerebral hemispheres will cause intense phagocytic activity (Das and Altman, 1971; Jones and Brownson, 1969). Macrophages as well as astrocytes assume phagocytic activity (Jones and Brownson, 1969; Jones and Gardner, 1976; Maruyama and D'Agostino, 1967).

ULTRASTRUCTURAL EXAMINATION

Ultrastructural overview of the cerebellar cortex

In 10 day control mice we found many granule cells present in their definitive location (Figs. 3A, 4A, 5A). Ultrastructurally, numerous parallel fibers with varicosities containing synaptic vesicles and parallel fiber-Purkinje cell contacts within the molecular layer (Figs. 10 and 11) like those previously reported by del Cerro and Snider (1972) and Larramendi (1969) were also present. Occasional synaptic contacts have been reported on cells located beneath the external differentiating cell layer as early as the first postnatal day (del Cerro and Snider, 1972). Jones and Gardner (1976) observed a few parallel fiber-Purkinje cell dendritic spine synapses at two, three, and five days postnatally in Swiss albino mice. From days six to eleven, the presence of many parallel fiber-Purkinje cell dendritic spine synapses have been confirmed (Hirano and Dembitzer, 1974; Rakic and Sidman, 1973c). MAM has been shown to selectively destroy cells in the external differentiating layer of the cerebellum when injected on the first postnatal day. This results in a numerical decrease in

granule cell parallel fibers as well as their parallel fiber-Purkinje cell contacts (Jones, et al., 1973; Chanda, et al., 1975). We observed some areas of the molecular layer in 10 day MAM-injected mice that were devoid of parallel fibers (Fig. 15A). Jones and other researchers have reported similar observations in mice, rats and hamsters when injected with MAM or cycasin (Hirano, et al., 1972; Hirano and Jones, 1972; Jones, et al., 1972, 1973; Shimada and Langman, 1970; Woodward, et al., 1975). Parallel fiber reduction has also been noted in various animals with: chronic alcoholic consumption (Bauer-Moffett and Altman, 1975), a fetal virus infection of panleukopenia (Herndon, et al., 1971; Llinas, et al., 1972); x-ray exposure (Altman and Anderson, 1971, 1972), and a genetic mutation (Hirano and Dembitzer, 1973, 1975; Mouren-Mathieu and Colonnier, 1969; Sotelo, 1973).

Presence of naked Purkinje cell spine specializations

The presence of naked Purkinje cell dendritic spine specializations surrounded by a Bergmann astroglial matrix in 10 day control and MAM-injected mice has raised many questions pertaining to their development. The mechanism, the sequence of events leading to the formation, and the durability of naked spine specializations have been the subjects of many investigations, including this one.

Past investigators have assumed that the formation of pre- and postsynaptic membrane specializations have been preceded by the contact between the pre- and postsynaptic

elements (Bloom, 1970; Bunge, Bunge, and Peterson, 1967; Larramendi, 1969). Since then, naked Purkinje cell dendritic spine specializations have been shown to differentiate in the absence of parallel fibers (Altman and Anderson, 1972; Woodward, et al., 1975) caused by viral infection with panleukopenia (Herndon, et al., 1971; Llinas, et al., 1972), gene mutations (Hirano and Dembitzer, 1973, 1975; Sotelo, 1973, 1975), focal lesions of the parallel fibers (Mouren-Mathieu and Colonnier, 1969), or MAM (Hirano, et al., 1972; Hirano and Jones, 1972; Jones, et al., 1973; Woodward, et al., 1975). Electron microscopic studies of cultures of normal mouse cerebellum have also resulted in the observation of naked Purkinje cell dendritic spine specializations (Calvet, et al., 1974; Seil and Herndon, 1970; Kim, 1975). Larramendi (1969, bottom right figure of plate 8, page 815) illustrated a naked Purkinje cell dendritic spine specialization surrounded by a Bergmann astroglial matrix in the 14 day normal mouse. The present study has also demonstrated naked Purkinje cell dendritic spine specializations surrounded by a Bergmann astroglial matrix (Fig. 13). Thus the hypothesis that presynaptic contact is necessary for postsynaptic element formation has been shown to be invalid.

In the absence of evidence of degeneration of presynaptic terminals in either group of mice this study would appear to strengthen the hypothesis that Purkinje cell dendritic spine specializations do not require permanent

presynaptic contact by parallel fibers for their development.

Hirano and Dembitzer (1975) concluded from research on the Weaver mouse, that Purkinje cell "dendritic spines do not seem to require a one-to-one induction of a presynaptic element," but they also suggest that the dendritic spines may be induced by some type of general stimulus. Sotelo (1975) suggests that not only postsynaptic densities, but presynaptic vesicular grids can develop in "the apparent absence of the pre- or postsynaptic elements respectively." Besides the appearance of naked Purkinje cell dendritic spine specializations due to pathologic factors, de novo differentiation of postsynaptic sites has been reported in the normal differentiating olfactory bulbs (Hamori, 1973; Palacios and Brinceno, 1972) and by Larramendi (1969) in 14 day mice. Thus many studies, including this one substantiate the hypothesis of de novo spine formation (Hirano, et al., 1972; Hirano and Jones, 1972; Jones and Gardner, 1976; Kim, 1975).

Durability of naked Purkinje cell dendritic spine specializations

Naked Purkinje cell dendritic spine specializations have been reported to be durable structures remaining intact after degeneration of the presynaptic element (Hamori, 1968, 1973; Herndon, 1968; Herndon, et al., 1971; Hirano and Dembitzer, 1975; Llinas, et al., 1972; Sotelo, 1973, 1975).

A pilot study in saline and MAM-injected mice also has revealed the presence of naked Purkinje cell dendritic spine specializations in 24 and 100 day saline-injected Swiss albino mice (Hartkop, unpublished; Appendix B). In the light of recent research (Sotelo, 1975), this research, and our pilot experiment, naked Purkinje cell dendritic spine specializations appear to persist throughout life surrounded by a Bergmann astroglial matrix. This research supports Sotelo's (1975) suggestion that naked Purkinje cell dendritic spine specializations are autonomous in their appearance and stability. The hypothesis of independent development and maintenance of naked Purkinje cell dendritic spine specializations is also supported.

Growth cones

Growth cones were observed within all saline-injected 10 day mice and only one of the five MAM-injected mice. del Cerro and Snider (1968) hypothesized that growth cones precede Purkinje cell dendritic spine formation and others have shown evidence that growth cones do precede the formation of axons and dendrites (Johnson and Armstrong-James, 1970; Skoff and Hamburger, 1974). The retardation of development of the cerebellar cortex in 10 day MAM-injected mice, observed macroscopically and photomicroscopically, is further substantiated by the ultrastructural observation of the presence of growth cones in only one out of five 10 day MAM-injected mice.

Necrotic debris

Necrotic debris has been observed within persistent or regenerating external differentiating cells as well as in degenerating cells 10 days following MAM-administration. Previously, necrotic debris has not been reported within the cerebellar cortex after five postnatal days in MAM-injected mice (Jones, et al., 1972a, 1973) but has been observed within Golgi cells from normal 10 day mice (Larramendi, 1969), and in normal fetuses (Maruyama and D'Agostino, 1967). Degeneration and necrosis in certain cases is considered to be a normal process (Maruyama and D'Agostino, 1967). In the case of the 10 day MAM-injected mice, the persistence of necrotic debris observed within the Bergmann astroglial processes may signify continued degeneration of the external differentiating cells induced by MAM-administration or a delayed response to injury.

Whorls

Membranous whorls composed of smooth concentric membranes were occasionally observed within astrocytes of 10 day mice of both groups (saline or MAM-injected). They were encountered in both foot processes and bulbous terminals of Bergmann astroglia as well as within Bergmann astroglial fibers (Fig. 16A). The concentric lamellated whorls are composed of collapsed cisternae that appear to be derived from endoplasmic reticulum (Palay and Chan-Palay, 1974; Sotelo and Palay, 1971). They resemble concentric

laminar membranes observed in axon terminals. Smooth membranes have been shown to have the capability of producing intracellular concentric whorls and have been shown to occur also in a variety of non-neural tissues (Sotelo and Palay, 1971). Sotelo and Palay (1971) also suggest that the overproduction of smooth membranes is characteristic of developing, growing, or regenerating processes which appear to be present in the 10 day saline and MAM-injected mice.

In contrast, spirals without any type of cistern separating the lamellar membranes, have also been observed within saline and MAM-injected mice (Fig. 16B). Larramendi (del Cerro and Snider, 1969, discussion) and Chan-Palay (1973) believe that this is a fixation artifact, while del Cerro and Snider (1969) showed similar structures in Purkinje cell dendrites and attributed their presence to a toxic Dilantin effect. The formation of these spirals still remains unresolved.

SUMMARY AND CONCLUSIONS

Previous studies have shown the usefulness of methylazoxymethanol glucoside (cycasin), and its derivative methylazoxymethanol acetate (MAM) as aids in the understanding of normal and abnormal cerebellar differentiation. In the present study of the postnatal Swiss albino mouse cerebellum, attention was directed towards the differentiation of synaptic structures as well as the physical, histological and ultrastructural alterations on the tenth postnatal day. Physically, the MAM-treated 10 day mice were more immature than the saline-treated control mice. The MAM-treated mice weighed less, exhibited less hair and an abnormal postural stance. An evaluation of the midsagittal surface area of the vermis, revealed an average

MAM-treated mice weighed less, exhibited less hair and an abnormal postural stance. An evaluation of the midsagittal surface area of the vermis, revealed an average
the Purkinje cell dendrites in 10 day MAM-treated mice. This was attributed to the paucity of external differentiating and internal granule cells. The lateral processes of the Golgi epithelial (Bergmann) cells were reduced in length, passed in an oblique direction towards the pial-glial membrane, and contained fewer than normal warty excrescences. Ultrastructurally, in 10 day control mice many granule cells were present in their definitive location with numerous parallel fiber-Purkinje cell contacts and

growth cones in the molecular layer. Naked Purkinje cell dendritic spines with postsynaptic spine specializations were observed in both control and treated mice. No evidence of degeneration of presynaptic terminals was seen in either group (saline or MAM-injected mice).

By demonstrating naked Purkinje cell dendritic spine specializations in control and treated mouse cerebellums during early synaptogenesis, this study supports the hypothesis of de novo spine formation. Because of the element of repair and regeneration of granule cells shown, it is possible that after the tenth postnatal day, transient parallel fiber-Purkinje cell contacts form and contribute to the larger number of naked Purkinje cell postsynaptic specializations noted on the twenty-fifth postnatal day. Further studies in this time interval will be necessary to examine this possibility.

APPENDIX

APPENDIX A

EXPERIMENTAL PROCEDURES

PROCUREMENT AND INJECTIONS OF MICE

The laboratory materials consisted of a Mettler balance for weighing the mice, two Unimetrics syringes calibrated to deliver 0.05 ul, two extra cages for separating the control (saline-injected) and MAM-injected mice, microforceps, microscissors and a dissecting microscope to aid in marking the mice for separate identification.

Ten litter-mates were randomly selected for alternate injections of either MAM or saline. A mouse was then selected at random from these litter-mates, and the data related to the general activity, fur, tremor, climbing abilities (ability to climb the cage walls or rim of the scale plate), righting abilities (to resume an upright position within a certain time) and leg posture was recorded (See Appendix A charts 3,4). After weighing the mouse, MAM (0.05 ul/gm body weight) was injected subcutaneously. Next a toenail designating identification number was removed (Appendix A, Fig. 17). The second litter-mate (control) was physically examined, weighed, data recorded, and injected with saline (0.05 ul/gm body weight). A toenail designating the same number as its litter-mate was removed and all data was recorded. The

control mice, five from each of the first two litters injected with saline (a total of 10 mice) were placed in a plastic shoebox cage containing pinechips with a foster mother. The MAM-injected mice were housed separately from the controls.

Since dams tend to cannibilize sick pups, especially when disturbed, the cages were not cleaned for the first 25 days.

Chart 3. PHYSICAL EXAM RATING SCALE

Activity	none	slow	normal	fast
Tremor	great deal	little	none	
Fur	scruffy	none	smooth	
Climbing	none	slow	normal	fast
Righting	none	slow 16 - 30*	fast 0 - 15*	
Leg Posture	abnormal		normal	
RATING SCALE USED ON FORMS	1	2	3	4

* time in seconds

Chart 4. A portion of the record sheet used for mice

INJECTION RECORD

DATE OF INJECTION_____ DATE OF SACRIFICE_____ MAM or

AGE AT INJECTION_____ AGE AT SACRIFICE_____ SALINE

LITTER #	ANIMAL #	SEX	WT.(gms) at INJECTION	PHYSICAL EXAM AT INJECTION
				ACTIVITY_____ TREMOR_____ FUR_____ RIGHTING_____ CLIMBING_____ LEG POSTURE_____ COMMENTS_____

Figure 17. TOE MARKING SYSTEM FOR ZERO - DAY MICE

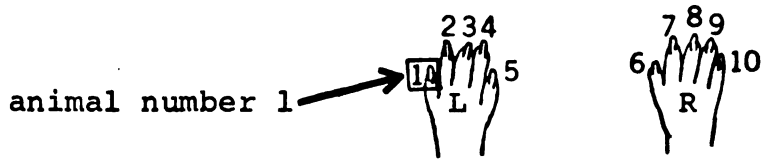

The toes are cut behind the toenail to remove the nail and nailbed, but not the rest of the toe. With practice, the toenail can be removed without any bleeding. The figure above represents the hind feet of a mouse lying prone with its head toward the top of the page.

A video tape has been prepared showing the equipment and the procedures for injection and identification described above (time, approximately 10 minutes). An outline of the tape contents follows.

INJECTION TECHNIQUE FOR NEWBORN SWISS ALBINO MICE

THOMAS HENRY HARTKOP, DEPARTMENTS OF ANATOMY AND PATHOLOGY

A. Introduction
    1. Materials
    2. Physical examination rating scale
    3. Identification system (toe marking chart)
    4. Injection chart
B. Weighing procedure, physical examination, injection record
C. Method of filling syringes
D. Identification system continued (removal of toenail)
E. Injection procedure
F. Brief review

PERFUSION TECHNIQUE

The perfusion techniques used were modified from the methods described by Pàlay and Chan-Palay, 1974. The modifications were made in order to reduce the osmolality of the fixative, rinse solution and postfixative (Maser, 1974). The concentration of paraformaldehyde was reduced from 1% to 0.5%, thus reducing the osmolality of the fixative from 760 mOsM to 520 mOsM.

The rinse solution described by Palay and Chan-Palay used eight grams of dextrose per 100 ml of solution which has a resulting osmolality of 710 mOsM. Since this was considered too high (an optimum fixative is slightly hypertonic, between 400 - 630 mOsM, Peters, 1970), the amount of dextrose added was reduced to four grams per 100 ml of solution which reduced the measured osmolality to 453 mOsM.

In preparing the double strength buffer for the osmium tetroxide, 3.5 gm of dextrose per 50 ml of solution was added instead of the recommended seven grams of dextrose. This effectively reduced the osmolality from 680 mOsM to 470 mOsM.

Two video tapes have been prepared showing two similar methods for perfusing mice. Tape A shows the techniques for perfusing adult mice, while Tape B shows the techniques for perfusing 10 day mice and embedding sections. These tapes are available through the Departments of Anatomy and

Pathology at Michigan State University, as instructional aids for students, researchers and technicians. An outline of the tape contents follows.

PERFUSION TECHNIQUE. TAPE A - ADULT SWISS ALBINO MICE

BY THOMAS HENRY HARTKOP, DEPARTMENTS OF ANATOMY AND PATHOLOGY

A. Introduction
    1. Materials
    2. Overview of perfusion
B. Weighing mice
C. Data sheet and explanation
D. Injection of Anesthetic
E. Dissection of Thorax
    1. Heparinization
    2. Perfusion begins
    3. Perfusion ends after 30 minutes
F. Dissection of skull for removal of cerebellum
G. Overview of rinsing, postfixing, dehydration, infiltration and embedding of tissue for electron microscopy.

PERFUSION AND EMBEDDING TECHNIQUES. TAPE B - 10 DAY MICE

BY THOMAS HENRY HARTKOP, DEPARTMENTS OF ANATOMY AND PATHOLOGY.

A. Introduction
   1. Materials
   2. Comparison between 10 day control and MAM injected mice.

B. Weighing mice

C. Techniques for filling the syringes with Nembutal, sodium nitrite and Heparin.

D. The anesthesia of a 10 day mouse with an intraperitoneal injection of Nembutal.

E. Dissection of the Thorax.
   1. Injection of Heparin and sodium nitrite into the left ventricle.
   2. Perfusion begins.
   e. Perfusion ends after 20 - 30 minutes.

F. Dissection and removal of head and leaving in the perfusate at 4 C overnight.

G. Materials for dissecting the head.

H. Dissection of head and removal of cerebellum.

I. Dehydration of tissue and infiltration into 100% Epon-araldite.

J. Embedding tissue in Beam capsules.
   1. Cutting larger parasagittal sections into smaller pieces.
   2. Comparison of parasagittal sections in saline

and MAM injected mice.

3. Placement of tissue in Beam capsules.
4. Repositioning tissue sections so that parasagittal sections will result when the blocks are cut.

Additional data are recorded on a perfusion record needed for later analyses (see Chart 5).

Chart 5. PERFUSION RECORD

Litter #	EXAMINATION	
	ACTIVITY	ANESTHETIC & AMT.
Animal #	FUR	TIME GIVEN
	TREMOR	HEPARIN AMT.
Treatment	CLIMBING ABILITIES	PERFUSATE
		TIME STARTED
Sex	LEG POSTURE	TIME STOPPED
		EAR COLOR
Weight	COMMENTS	MOUTH COLOR
		NOSE COLOR
Age		RUNNY NOSE
		TAIL COLOR

Summary of perfusion

Impressions

PERFUSED BY _____ **DATE** _____

Chart 6. ELECTRON MICROSCOPIC DATA SHEET

Comments - listed by BLOCK #, GRID #,

PHOTO #, AND DATE.

ANIMAL NUMBER _____

TREATMENT _____

AGE _____

PRESYNAPTIC REGION

Presynaptic terminals (varicosities) _____

Naked presynaptic varicosities _____

Synaptic vesicles in varicosities _____

Spines on Pc d _____

Naked spines on Pc d with Pt _____

Postjunctional dense bodies _____

Microtubules _____

Cisternae in Pc d _____

Whorls _____

Growth cones _____

Normal cleft _____

Normal pf-Pc d synapse _____

KEY: Synaptic vesicles
R = round synaptic vesicles
P = pleomorphic
D = dense bodies in larger vesicles
\+ = present or observed
\- = not observed or present
Pc d = Purkinje dendrite
Pt = postsynaptic thickening
pf = parallel fiber

MORPHOMETRIC EVALUATION OF SAGITTAL SECTIONS OF VERMIS

Whole sagittal tissue sections of the vermis, cut from blocks were projected through a Bausch and Lomb Microprojector at a magnification of 22 X and the outline of the vermis traced (1 mm^2 on a slide equals 484 mm^2 on the projected surface at 22 X). By placing a previously prepared transparent Dot Grid (1 dot represents 4.3264 mm^2, Fig. 18) over the tracings, counting the number of dots within the tracing, multiplying this times 4.3264 mm^2 (the surface area represented by one dot on the Dot Grid), then dividing this by 484 (the magnification factor for 22 X), results in the two dimensional area of the section of tissue on the glass slide in mm^2. This procedure was modified from the method according to Weibel, E.R., et al. (1966).

Figure 18. HARTKOP COUNTING CHAMBER - 2-10-76

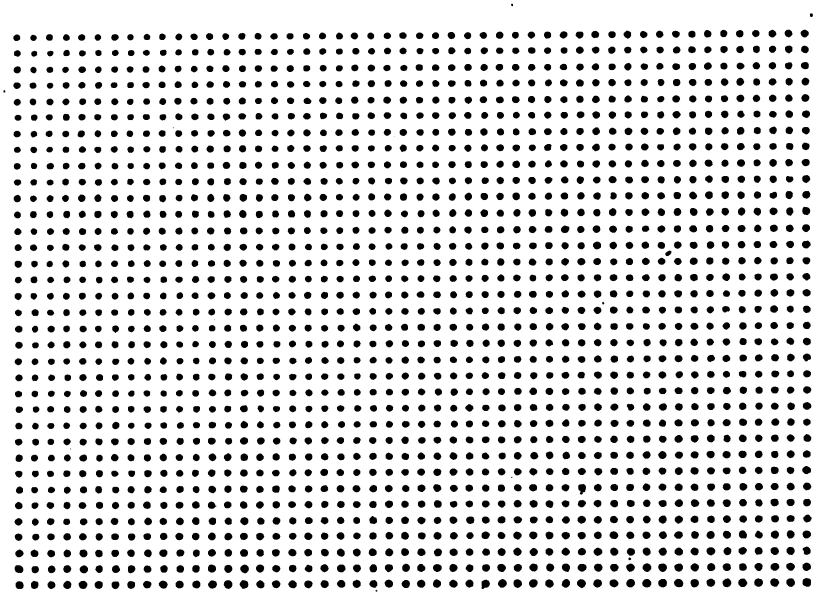

HARTKOP ELECTRON MICROSCOPIC MEASUREMENT NOMOGRAPH

The measurement of structures in micrographs is accomplished with the use of an Electron Microscopic Measurement Nomograph that I developed to reduce the time involved comparing structures in micrographs of different magnifications (Fig. 19). The Nomograph has four scales of magnification (0 - 1,600 X, 0 - 16,000 X, 0 - 160,000 X, 0 - 1,600,000 X) that can measure objects in microns for the lower magnifications and Angstroms for the highest magnification. Knowing the magnification of the micrograph, place one side of the object to be measured on the baseline, aligning it with the magnification listed on the horizontal scale. Follow the vertical line at that magnification to the other side of the measured structure. Follow the closest diagonal line to the right and read the size of the structure in the appropriate column (within the magnification range).

Figure 19. HARTKOP ELECTRON MICROSCOPIC MEASUREMENT NOMOGRAPH (2/3 scale)

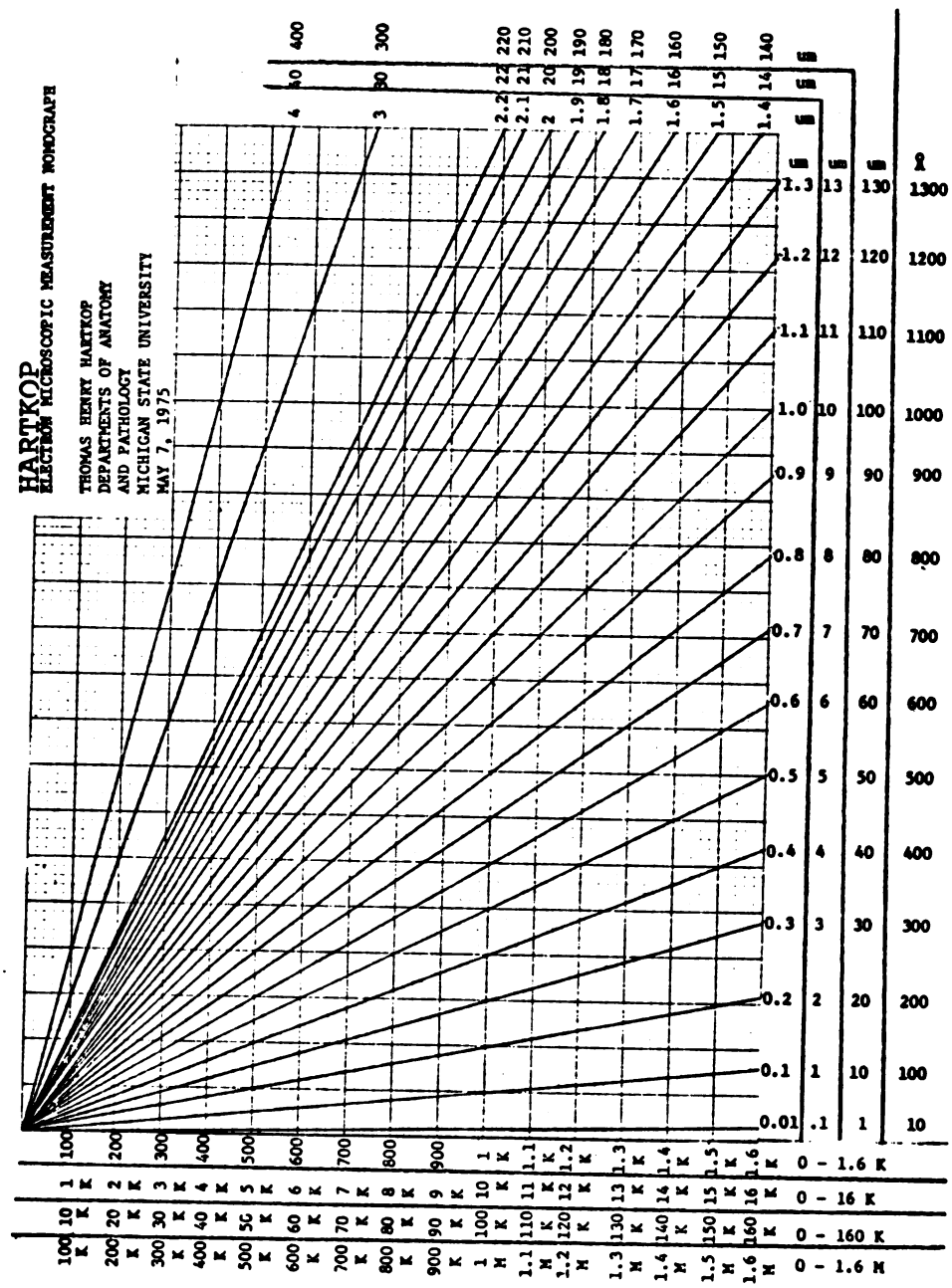

APPENDIX B - PILOT STUDIES

MATERIALS AND METHODS

Newborn Swiss albino mice, Webster strain, (obtained from Spartan Animal Research, Haslett Michigan) were selected randomly from many litters (reduced to 10), examined, weighed, marked for identification and injected with methylazoxymethanol acetate (MAM) (0.05 ul/gm body weight) or saline (0.05 ul/gm body weight) (Appendix A). Both groups (saline and MAM-injected) of mice were housed in plastic shoe box cages containing pinechips at controlled room temperature. Humidity and a standard light-dark cycle were maintained. Mice in each group were sacrificed at 0, 25, and 100 days of age after they were weighed again. Three mice from each group (saline and MAM-injected) at each time period were anesthetized with Nembutal (sodium pentobarbital, 0.05 mg/gm body weight). After thoracotomy and exposure of the heart, heparin (300 units/animal) was injected into the left ventricle. The mice were then perfused (Appendix A) with a 3% glutaraldehyde fixative in a 0.1 M cocodylate buffer, adjusted to pH 7.4. After perfusion for 30 minutes, the cerebellum was removed, postfixed in 1% osmium tetroxide (OsO_4) in 0.1 M cacodylate buffer for thirty minutes, dehydrated through graded alcohols, and embedded in Epon-araldite. One micron thick sections were stained with 1% toluidine blue, while thin sections were stained with lead citrate for 1 minute and uranyl acetate for 30 minutes.

Ultrastructurally, the Purkinje cell dendrites, granule cell parallel fibers and their synapses were qualitatively assessed for the presence or absence of naked pre- or post-synaptic elements with the use of a Philips 201 electron microscope. The structures assessed were: naked Purkinje cell dendritic spines with a postsynaptic thickening, naked pre-synaptic varicosities, and parallel fiber-Purkinje cell synapses.

RESULTS

Preliminary ultrastructural examination

Naked Purkinje cell dendritic spines with postsynaptic thickenings were not observed at postnatal day zero in saline and MAM-injected mice. At 25 and 100 postnatal days, naked Purkinje cell dendritic spines with postsynaptic thickenings were occasionally observed in MAM-injected mice, and rarely observed in saline-injected mice (Fig. 20). No parallel fiber-Purkinje cell dendritic spine synapses were observed at day zero but were present in both groups (saline and MAM-injected) at postnatal day 25 and 100. No naked parallel fiber varicosities were observed at 0, 25, and 100 postnatal days in saline and MAM-injected mice.

COMMENTS ON FIXATION

In the course of pilot studies, I realized the fixative and buffer (3% glutaraldehyde in a 0.1 M cacodylate buffer at pH 7.4) produced large extracellular spaces within the

cerebellar cortex of young animals (0 - 10 postnatal days) which was reduced in adults.

Many factors have be evaluated when designing a fixative, rinse solution or postfixative. They are the osmolality, pH, temperature, fixative concentration post-fixative concentration, buffer concentration as well as salts added to reduce any salt gradients.

The osmolality of the plasma is around 280 - 320 mOsM. Shultz and Karlsson (1965) reported that hypotonic solutions (below 280 mOsM) or isotonic solutions (280 - 320 mOsM) cause gross swelling of the brain and poor preservation on the ultrastructural level. A hypertonic solution around 1200 mOsm causes gross brain shrinkage while a moderate hypertonic solution (400 - 620 mOsM) results in subtle shrinkage and does not cause an excessive extracellular space (Schultz and Karlsson, 1965; Sumi, 1969).

The pH should be close to that physiologically measured in the plasma (Maser, et al., 1967). The temperature of the perfusate has not been throughly described but, it does not seem to have a drastic effect on the ultrastructure (Hayat, 1972). Therefore, a fixative/perfusate should be slightly hypertonic (400 - 620 mOsM) at a pH near 7.4 (Maser, et al., 1967).

In order to produce a perfusate with an osmolality of 400 to 620 mOsM at pH 7.4 a 1 - 2% gluteraldehyde solution

will have to be used with a 0.1 M phosphate buffer (210 mOsM, which is optimum) (Maser, et al., 1967). The use of two aldehydes in combination (glutaraldehyde and paraformaldehyde) has also been used with excellent results (Palay and Chan-Palay, 1974). As a result, the new perfusate that I designed used a 1% glutaraldehyde (100 mOsM), 0.5% paraformaldehyde (200 mOsM) combined perfustate in a .12 M phosphate buffer (220 mOsM) with 0.02 mM calcium chloride (5 - 10 mOsM) added to reduce any salt gradient (modified from Palay and Chan-Palay, 1974).

The rinse solutions osmolality has also been thought to be critical. In trying to design one near an osmolality of 400 - 620 mOsM, dextrose was added to increase the osmolality of the .12 M phosphate buffer (220 mOsM) to 460 mOsM. Calcium chloride was also added to reduce any salt gradient that may exist (Maser, et al., 1967). A normal postfixative (1% OsO_4 in a 0.1 M cacodylate buffer) has an osmolality of 240 mOsM. This is hypotonic. In order to raise the osmolality to 400 to 620 mOsM, destrose was also added.

Therefore, in the new fixative used in the body of this thesis, the fixative(520 mOsM), rinse solution (460 mOsM) and the postfixative (470 mOsM) osmolalities were drastically altered to reduce the extracellular space as well as other artifacts.

Figure 20. A naked Purkinje dendritic spine (NS) with a postsynaptic spine specialization (arrow) can be observed on a Purkinje cell dendrite (Pc d) surrounded by a Bergmann glial matrix (GL) in this 100 day saline-injected mouse cerebellar cortex. Note the paucity of parallel fibers in this exceptional area within the middle one-third of the molecular layer within the declive. This long thin naked spine (NS) is also similar to those observed within the 25 day saline injected mice. Epon-araldite embedded, grids stained with uranyl acetate and lead citrate, 18,900 X.

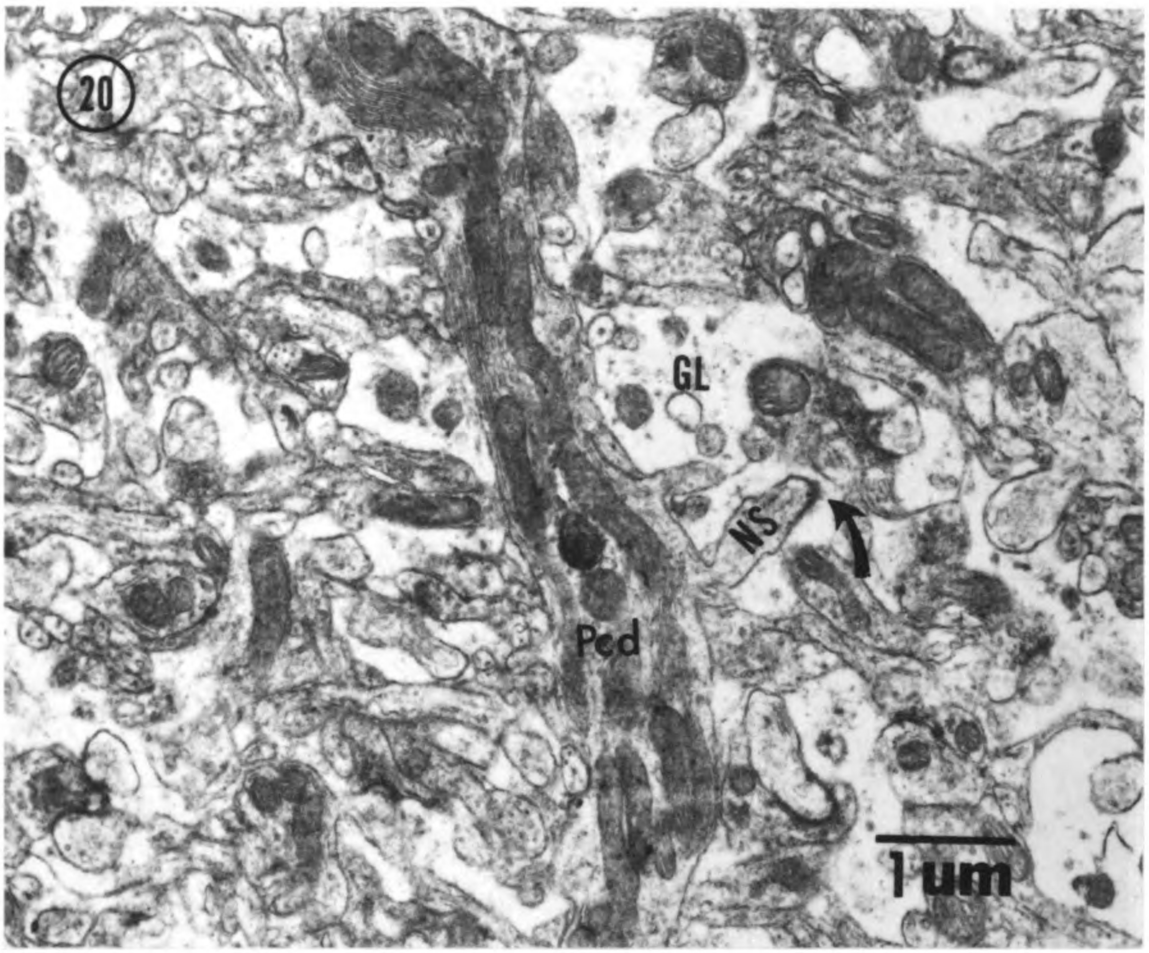
20
GL
NS
Ped
1um

BIBLIOGRAPHY

BIBLIOGRAPHY

Akert, K., K. Pfenninger, C. Sandri, and H. Moor. 1972. Freeze etching and cytochemistry of vesicles and membrane complexes in synapses of the central nervous system, p. 67-86. In: G.D. Pappas and D.P. Purpura (Eds.) Structure and Function of Synapses. Raven Press, New York.

Altman, J., W.J. Anderson, and K.A. Wright. 1967. Selective destruction of precursors of microneurons of the cerebellar cortex with fractionated low-dose x-rays. Exp. Neurol. 17:481-497.

Altman, J., W.J. Anderson, and K.A. Wright. 1969. Early effects of x-irradiation of the cerebellum in infant rats: Decimation and reconstitution of the external granular layer. Exp. Neurol. 24:196-216.

Altman, J., and W.J. Anderson, and M. Strop. 1971. Retardation of cerebellar and motor development by focal x-irradiation during infancy. Physiol. Behav. 7:143-150.

Altman, J., and W.J. Anderson. 1971. Irradiation of the cerebellum in infant rats with low-dose x-ray histological and cytological effects during infancy and adulthood. Exp. Neurol. 30:492-509.

Altman, J., and W.J. Anderson. 1972. Experimental reorganization of the cerebellar cortex. I. Morphological effects of elimination of all microneurons with prolonged x-irradiation started at birth. J. Comp. neurol. 146:355-406.

Altman, J., and W.J. Anderson. 1973. Experimental reorganization of the cerebellar cortex. II. Effects of elimination of most microneurons with prolonged x-irradiation started at four days. J. Comp. Neurol. 149:123-152.

Altman, J. 1975. Postnatal development of the cerebellar cortex in the rat. IV. Spacial organization of bipolar cells, parallel fibers and glial cells. J. Comp. Neurol. 163:427-447.

Anderson, W.J., and J. Altman. 1972. Retardation of cerebellar and motor development in rats by focal x-irradiation beginning at four days. Physiol. Behav. 8:57-67.

Bauer-Moffett, C., and J. Altman. 1975. Research note, ethanol-induced reductions in cerebellar growth of infants. Exp. Neurol. 48:378-382.

Bignami, A., and D. Dahl. 1974. The development of Bergmann glia in mutant mice with cerebellar mutations: Reeler, Staggerer and Weaver. Immunofluroescence study with antibodies to the glial fibrillary acidic protein. J. Comp. Neurol. 155:219-230.

Bloom, F.E. 1970. The formation of synaptic junctions in developing rat brain, p. 101-120. In: G.D. Pappas and D.P. Purpura (Eds.) Structure and Function of sySynapses. Raven Press, New York.

Bunge, M.B., R.P. Bunge, and E.P. Peterson. 1967. The onset of synapse formation in spinal cord cultures as studied by electron microscopy. Brain Res. 6:728-749.

Caddy, K.W.T., and T.J. Biscoe. 1975. Preliminary observations on the cerebellum in the mutant mouse Lurcher. Brain Res. 91:276-280.

Calvet, M., M. Drian, and A. Privat. 1974. Spontaneous electrical patterns in cultured Purkinje cells grown with an antimitotic agent. Brain Res. 79:285-290.

Chan-Palay, V. 1973. Neuronal plasticity in the cerebellar cortex and lateral nucleus. Z. Anat. Entwicki. Gesch. 142:23-35.

Chanda, R., D.J. Woodward, and S. Griffin. 1973. Cerebellar development in the rat after early postnatal damage by methylazoxymethanol: DNA, RNA, and protein during recovery. J. Neurochem. 21:547-555.

Chanda, R., D.J. Woodward, and W.S.T. Griffin. 1975. Deoxyribonucleases in developing and adult rat cerebellum: Transient and long duration actions of methylazoxymethanol. J. Neurochem. 24:723-727.

Cotman, C.W., and G.A. Banker. 1974. The making of a synapse, p. 1-62. In: S. Ehrenpreis and I.J. Kopin (Eds.) Rev. Neurosci. Vol. 1. Raven Press, New York.

Das, G.P., and J. Altman. 1971. Transplanted precursors of nerve cells: Their fate in cerebellums of young rats Science 173:637-638.

del Cerro, M.P., and R.S. Snider. 1968. Studies on the developing cerebellum: Ultrasturcture of growth cones. J. Comp. Neurol. 133:341-362.

del Cerro, M.P., and R.S. Snider. 1969. Cerebellar alterations resulting from Dilantin intoxication: An ultrastructural study, p. 380-411. In: W.S. Fields and W.D. Willis (Eds.) The Cerebellum in Health and Disease. Warren H. Green Inc., St. Louis.

del Cerro, M.P., and R.S. Snider. 1972. Studies on the developing cerebellum. II. The ultrastructure of the external granular layer. J. Comp. Neurol. 144:131-164.

Dvorak, K. and J. Bucek. 1970. Postnatal differentiation of the Golgi apparatus and the dendrites of Purkinje cells of the rat cerebellum. Z. Zellforsch. 111:51-63.

Gray, E.G. 1959. Axosomatic and axodendritic synapses of the cerebral cortex: An electron microscopic study. J. Anat. Lond. 93:420-433.

Gray, E.G. 1961. The granule cells, mossy synapses and Purkinje spine synapses of the cerebellum: Light and electron microscope observations. J. Anat. 95:345-356.

Gray, E.G. 1966. Problems of interpreting the fine structure of vertebrate and invertebrate synapses. Int. Rev. Gen. Exp. Zol. 2:139-170.

Gray, E.G., and R.W. Guillery. 1966. Synaptic morphology in the normal and degenerating nervous system. Int. Rev. Cytol. 19:111-182.

Ganote, C.E., and A.S. Rosenthal. 1968. Characteristic lesions of methylazoxymethanol-induced liver damage. A comparative ultrastructural study with dimethylnitrosamine hydrazine sulfate and carbon tetrachloride. Lab. Invest. 19:382-398.

Grondin, G., T. Sharkey, M. Jones, A. Sculthorpe, and W. Taylor. 1975. Postnatal cerebellar hypoplasia and dysfunction following methylazoxymethanol acetate treatment. Proc. Soc. Exp. Biol. Med. 148:156-159.

Hamori, J. 1968. Presynaptic-to-presynaptic axon contacts under experimental conditions giving rise to rearrangement of synaptic structures, p. 71-80. In: C. Euler (Ed.) Structure and Function of Inhibitory Neuronal Mechanisms. Pergamon, New York.

Hamori, J. 1969. Development of synaptic organization in the partially agranular and in the transneuronally atrophied cerebellar cortex, p. 845-848. In: R. Llinas (Ed.) Neurobiology of Cerebellar Evolution and Development. Amer. Med. Assoc., Chicago, Ill.

Hamori, J. 1973. The inductive role of presynaptic axons in the development of postsynaptic spines. Brain Res. 62:337-344.

Hayat, M.A. 1970. Principles and Techniques of Electron Microscopy. Van Nostrand Reinhold Company, New York.

Herndon, R.M. 1964. The fine structure of the rat cerebellum II. The stellate neurons, granule cells and glia. J. Cell. Biol 23:277-293.

Herndon, R.M. 1968. Thiophen induced granule cell necrosis in the rat cerebellum: An electron microscopic study. Exp. Brain Res. 6:49-68.

Herndon, R.M., G. Margolis, and L. Kilham. 1971. The synaptic organization of the malformed cerebellum induced by perinatal infection with the feline panleukopenia virus (PLV). II. The Purkinje cell and its afferents. J. Neuropath. Exp. Neurol. 30:557-570.

Hirano, A, H.M. Dembitzer, and M. Jones. 1972. An electron microscopic study of cycasin-induced cerebellar alterations. J. Neuropath. Exp. Neurol. 31:113-125.

Hirano, A., and M. Jones. 1972. Fine structure of cycasin-induced cerebellar alterations. Fed. Proc. 31:1517-1519.

Hirano, A., and H.M. Dembitzer. 1973. Cerebellar alterations in the Weaver mouse. J. Cell. Biol. 56:478-486.

Hirano, A., and H.M. Zimmerman. 1973. Aberrant synaptic development. Arch. Neurol. 28:359-366.

Hirano, A., and H.M. Dembitzer. 1974. Observations on the development of the cerebellum. J. Neuropath. Exp. Neurol. 33:354-364.

Hirano, A., and H.M. Dembitzer. 1975. The fine structure of Staggerer cerebellum. J. Neuropath. Exp. Neurol. 34:1-11.

Hirono, I., and C. Shibuya. 1967. Induction of a neurological disorger by cycasin in mice. Nature 216:1311-1312.

Hirono, I. 1969. Carcinogenicity and neurotoxicity of cycasin. Fed. Proc. 31:5, 1493-1497.

Hopewell, J.W. 1974. The permanent long-term effects of postnatal x-irradiation on the rat cerebellum. Acta Neuropathol. (Berl). 27:163-169.

Johnson, R., and M. Armstrong-James. 1970. Morphology of superficial postnatal cerebral cortex with special reference to synapses. Z. Zellerforsch. 110:540-558.

Jones, M.Z., and R.H. Brownson. 1969. Some qualitative aspects of the stratum granulosum in the postnatal rat hippocampus, p. 823-839. In: M.R., and D.H. Mahlum (Eds.) Radiation Biology of the Fetal and Juvenile Mammal. U.S. Atomic Energy Commission, Division of Technical Information, Washington, D.C.

Jones, M.Z. 1971. Cycasin-induced cerebellar pathology in the postnatal Swiss albino mouse. Amer. J. Path. 61:6a.

Jones, M.Z., M. Yang, and O. Mickelsen, 1972a. Effects of methylazoxymethanol acetate and methylazoxymethanol glucoside on the cerebellum of postnatal Swiss albino mouse. Fed. Proc. 31:1508-1511.

Jones, M., C. Sweeley, and M. Yang. 1972b. Lipid composition of the cerebellum and spinal cord in postnatal cycasin-treated Swiss albino mice: Preliminary observations. Fed. Proc. 31:1512-1516.

Jones, M., O. Mickelsen, and M. Yang. 1973. Methylazoxymethanol neurotoxicity, p. 91-114. In: H.M. Zimmerman (Ed.) Progress in Neuropathology, Vol II. Grune & Stratton, Inc. New York.

Jones, M., and E.M. Gardner. (1976) In press. Pathogenesis of methylazoxymethanol induced hypoplasia. J. Neuropath. Exp. Neurol. 35: no.4.

Kim, S.U. 1975. Formation of unattached spines on Purkinje cell dendrite in organotypic cultures of mouse cerebellum. Brain Res. 88:52-58.

Lane, P.W. 1964. Weaver, wv, recessive, p. 66-67. In: R. Sidman, M.C. Green, and S.H. Appel (Eds.) Catalog of Neurological Mutants of the Mouse. 1965. Harvard University Press, Cambridge, Mass.

Larramendi, L.M.H. 1969. Analysis of synaptogenesis in the cerebellum of the mouse, p. 803-844. In: R. Llinas (Ed) Neurobiology of Cerebellar Evolution and Development. Amer. Med. Assoc., Chicago.

Lauder, J.M., J. Altman, and H. Krebs. 1974. Some mechanisms of cerebellar foliation: Effects of early hypo- and hyperthyroidism. Brain Res. 76:33-40.

Llinas, R., D.E. Hillman, and W. Precht. 1972. Neuronal circuit reorganization in mammalian agranular cerebellar cortex. J. Neurobiol. 4:69-94.

Llinas, R., 1975. The cortex of the cerebellum. Sci. Am. Jan. 56-71.

Luna, L.G. 1968. Manual of histological staining methods of the Armed Forces Institute of Pathology, Third Edition, McGraw-Hill Book Company, New York.

Margolis, G., and L. Kilham. 1970. Cerebellar ontogenetic patterns: Key to a virus code, p. 353-379. In: W.S. Fields and W.D. Willis (Eds.) The Cerebellum in Health and Disease. Warren H. Green Inc., St. Louis.

Maruyama, S., and A.N. D'Agostino. 1967. Cell necrosis in the central nervous system of normal rat fetuses. Neurol. 17:550-557.

Maser, M.D., T.E. Powel III, and C.W. Philpott. 1967. Relationships among pH, osmolarity and concentration of fixative solutions. Stain Tech. 42:175-182.

Matsumoto, H., and H.H. Higa. 1966. Studies in methylazoxymethanol, the aglycone of cycasin, methylation of nucleic acids in vitro. Biochem. J. 98:20c-22c.

Matsumoto, H., M. Spatz, and G.L. Laqueur. 1972. Qualitative changes with age in the DNA content of methylazoxymethanol-induced microencephalic rat brain. J. Neurochem. 19:297-306.

Meller, K. and P. Glees. 1969. The development of the mouse cerebellum. A Golgi and electron microscopic study. In: R. Llinas (Ed.) Neurobiology of Cerebellar Evolution and Development, p. 783-801. Amer. Med. Assoc., Chicago.

Mettler, F.A., and D.S. Sax. 1972. Cerebellar cortical degeneration due to acute azide poisoning. Brain 95:505-516.

Mouren-Mathieu, A.M., and M. Colonnier. 1969. The molecular layer of the adult cat cerebellar cortex after lesion of the parallel fibers: An optical and electron microscope study. Brain Res. 16:307-323.

Nagata, Y., and H. Matsumoto. 1969. Studies on methylazoxymethanol: Methylation of nucleic acids in the fetal brain. Proc. Soc. Exp. Biol. Med. 132:383-385.

Norman, R.M. 1940. Primary degeneration of the granular layer of the cerebellum: An unusual form of familial cerebellar atrophy occurring in early life. Brain 63:365-379.

Palacios Pru, E.L., and R.V. Mendoza Briceno. 1972. An unusual relationship between glial cells and neuronal dendrites in olfactory bulbs of Desmodus rotundas. Brain Res. 36:404-408.

Palay, S.L., and V. Chan-Palay. 1974, Cerebellar cortex: Cytology and organization. Springer-Verlag, New York.

Peters, A. 1970. The fixation of central nervous tissue and the analysis of electron micrographs of the neuropil, with special reference to the cerebral cortex, p. 56-76. In: W.J.H. Nauta and S.O.E. Ebbesson (Eds.) Contemporary Research Methods in Neuroanatomy. Springer-Verlag, New York.

Rakic, P. 1971. Neuron-glia relationships during granule cell migration in developing cerebellar cortex. A Golgi and electron microscopic study in Macacus Rhesus. J. Comp. Neurol. 147:283-312.

Rakic, P., and R.L. Sidman. 1973a. Weaver mutant mouse cerebellum: Defective neuronal migration secondary to abnormality of Bergmann glia. Proc. Nat. Acad. Sci. 70:240-244.

Rakic,P., and R.L. Sidman. 1973b. Sequence of developmental abnormalities leading to granule cell deficit in cerebellar cortex of Weaver mutant mice. J. Comp. Neurol. 152:103-132.

Rakic, P., and R.L. Sidman. 1973c. Organization of cerebellar cortex secondary to deficit of granule cells in Weaver mutant mice. J. Comp. Neurol. 152:133-162.

Reynolds, E.S. 1963. The use of lead citrate at high pH as an electron-opaque stain in electron microscopy. J. Cell Biol. 17:208-212.

Rezai, A., and H. Yoon. 1972. Abnormal rate of granule cell migration in the cerebellum of Weaver mutant mice. Develop. Biol. 29:17-26.

Sax, D.S., A. Hirano, and R.J. Shofer. 1968. Staggerer, a neurological murine mutant. An electron microscopic study of the cerebellar cortex in tye adult. Neurol. 18:1093-1100.

Seil, F.J., and R.M. Herndon. 1970. Cerebellar granule cells in vitro. A light and electron microscope study. J. Cell. Biol. 45:212-220.

Shank, R.C., and P.N. Magee. 1967. Similarities between the biochemical actions of cycasin and dimethylnitrosamine. Biochem. J. 105:521-527.

Sheehan, D.C., and B.B. Hrapchak. 1973. Theory and practice of histotechnology. C.V. Mosby Company, St. Louis.

Shimada, M. 1966. Cytokenetics and histogenesis of early postnatal mouse brain as studied by ^{3}H-thymadine autoradiography. Arch. Hist. Jap. 26:413-437.

Shimada, M., and J. Langman. 1970. Repair of the external granular layer of the hamster cerebellum after prenatal and postnatal administration of methylazoxymethanol. Teratology 3:119-134.

Shofer, R.J., G.D. Pappas, and D.P. Purpura. 1964. Radiation induced changes in morphological and physiological properties of immature cerebellar cortex, p. 476-508. In: Haley and Snider (Eds.) Response of the Nervous System to Ionizing Radiation. Little Brown, Boston.

Shultz, R.L., and U. Karlsson. 1965. Fixation of the central nervous system for electron microscopy by aldehyde perfusion. II. Effects of esmolarity, pH of perfusate, and fixative concentration. J. Ultrastruct. Res. 12:187-206.

Skoff, R.P., V. Hamburger. 1974. Fine structure of dendritic growth cones in embryonic chick spinal cord. J. Comp. Neur. 153:107-148.

Smith, R.L., T. Parks, and G. Lynch. 1974. A comparison of the role of the motor cortex in recovery from cerebellar damage in young and adult rats. Behav. Biol. 12:177-198.

Sotelo, C., and S.L. Palay. 1971. Altered axons and axon terminals in the lateral vestibular nucleus of the rat, possible example of axonal remodeling. Lab. Invest. 25:653-671.

Sotelo, C. 1973. Permanence and fate of paramembranous synaptic specializations in "mutants" and experimental animals. Brain Res. 62:345-351.

Sotelo, C., and J.P. Changeux. 1974. Trans-synaptic degeneration "en cascade" in the cerebellar cortex of Staggerer mutant mice. Brain Res. 67:519-526.

Sotelo, C., D.E. Hillman, A.J. Zamora, and R. Llinas. 1975. Climbing fiber deafferentiation: Its action on Purkinje cell dendritic spines. Brain Res. 98: 574-581.

Sotelo, C. 1975. Anatomical, physiological and biochemical studies of the cerebellum from mutant mice. II. Morphological study of cerebellar cortical neurons and circuits in the Weaver mouse. Brain Res. 94:19-44.

Spatz, M., W.J. Dougherty, and D.W.E. Smith. 1967. Teratogenic effects of methylazoxymethanol. Proc. Soc. Exp. Biol. Med. 124:476-478.

Sumi, S.M. 1969. The extracellular space in the developing rat brain: Its variation with changes in osmolarity of the fixative, method of fixation and maturation. J. Ulstruct. Res. 29:398-425.

Venable, J.H. and R.A. Coggeshall. 1965. A simplified lead citrate stain for use in electron microscopy. J. Cell Biol. 25:407-408.

Weibel, E.R., G.S. Kistler, and W.F. Scherle. 1966. Practical stereological methods for morphometric cytology. Rev. Cytol. 30:23-38.

Whiting, M.G. 1973. Toxicity of cycads. Econ. Bot. 17:269-302.

Woodward, D.J., B.J. Hoffer, and J. Altman. 1974. Physiological and pharmacological properties of Purkinje cells in rat cerebellum degranulated by postnatal x-irradiation. J. Neurobiol. 5:283-304.

Woodward, D.J., D. Bickett and R. Chanda. 1975. Purkinje cell dendritic alterations after transient developmental injury of the external granular layer. Brain Res. 97:195-214.

Zedeck, M.S., S.S. Sternbery, R.W. Poynter, and J. McGowen. 1970. Biochemical and pathological effects of methylazoxymethanol acetate, a potent carcinogen. Cancer Res. 30:801-812.